Title

Review of Molecular Dynamics Simulations of Phosphonium Ionic Liquid Lubricants

Journal

Tribology Letters, 70(2)

ISSN

1023-8883

Authors

Liu, Ting
Panwar, Pawan
Khajeh, Arash
et al.

Publication Date

2022-06-01

DOI

10.1007/s11249-022-01583-6

Peer reviewed

Review of Molecular Dynamics Simulations of Phosphonium Ionic Liquid Lubricants

Ting Liu[1], Pawan Panwar[1], Arash Khajeh[1], Md Hafizur Rahman[2], Pradeep L. Menezes[2] and Ashlie Martini[1*]

[1*]Department of Mechanical Engineering, University of California Merced, 5200 Lake Rd, Merced, 95343, CA, USA.
[2]Department of Mechanical Engineering, University of Nevada-Reno, 1664 N Virginia St, Reno, 89557, NV, USA.

*Corresponding author(s). E-mail(s): amartini@ucmerced.edu;

Abstract

Phosphonium ionic liquids (ILs) have various uses, including as environmentally benign lubricants and lubricant additives. The properties and behavior of these ILs depend on their chemical composition, i.e., cation and anion combination, and the operating conditions. One approach to understanding the relationships between composition, conditions, and lubricant-relevant properties is classical molecular dynamics simulation. Although this research area is still emerging, it is growing rapidly, so a review of the topic is timely. Here, we review force field-based molecular dynamics simulations of phosphonium ILs, with emphasis on physical, chemical, and thermal properties relevant to lubricants. Properties reported in previous studies are density, viscosity, self-diffusivity, ionic conductivity, heat capacity, and thermal stability, as well as interactions with other compounds, including H_2O and CO_2, and solid surfaces. The effects of anion and cation, as well as conditions such as temperature, on these properties are identified and analyzed in terms of anion-cation structure, orientation, and interactions. Finally, trends are summarized and opportunities for future research are identified.

Keywords: phosphonium ionic liquids, lubricants, lubricant additives, molecular dynamics simulations

Statements and Declarations The authors have no conflicts of interest to declare that are relevant to the content of this article.

1 Introduction

Ionic liquids (ILs) are room temperature liquid salts with melting point below 25°C that comprise cations and anions. ILs possess unique physico-chemical properties such as low vapor pressure, excellent thermal stability, high viscosity, high ion conductivity, wide electrochemical window, tunable polarity, etc. [1]. These properties make ILs useful for a diverse range of applications, including lubrication [2, 3].

ILs that have been considered for lubrication use many different anions, either organic or inorganic, and cations. However, the most common cations are ammonium-, phosphonium-, imidazolium-, or pyridinium-based. Among these, phosphonium ILs have been the focus of recent studies for several reasons. First, phosphonium ILs have been reported to exhibit lower wear and friction than synthetic and petroleum-based oils as well as ammonium and imidazolium ILs [4–9]. Phosphonium ILs have also better miscibility in mineral and synthetic base oil than their imidazolium and pyrrolidinium counterparts, which is important for the use of ILs as additives [10]. The lack of acidic protons makes phosphonium ILs more stable in strongly basic media and more thermally stable than ammonium ILs [11–13]. Superior resistance to corrosion and tribo-corrosion has also been reported for phosphonium ILs [14–16]. Finally, many halogen-free phosphonium ILs have been developed that are considered environmentally friendly [17–19], since they can be extracted from bio-based feedstock [3] and biodegradable [20–22]. They can also be recycled and reused without volume loss due to their non-volatility [23–25]. With these advantages, phosphonium ILs are leading candidates for lubricant applications [3, 23, 26, 27].

There are several types of phosphonium cations having the general chemical formula [PR_4], with R = H, alkyl, aryl, ester, and halide, etc. Frequently studied phosphonium cations are tetraalkylphosphonium,triarylphosphonium, methoxyalkyl-trialkylphosphonium, and more complicated forms like [4-(methoxycarbonyl)benzyl](triphenyl)phosphonium [28]. Snapshots of atomistic models of some common phosphonium cations are shown in Figure 1.

The physico-chemical properties of phosphonium ILs are tunable depending upon the combination of cation and anion employed. Generally, studies have shown that properties vary with the length and branching of the alkyl chains in the cation and the anion chemistry. Changes in properties in turn affect the performance of phosphonium ILs in different applications. Although there have been many investigations into relationship between IL properties and ion chemistry/structure, the selection of cation and anion for phosphonium ILs is still very much trial-and-error. To optimize phosphonium ILs for lubrication, a full understanding of the relationship between IL chemistry/structure and material properties is required.

Atomistic simulations are important numerical methods for the investigation of magnetic, electronic, chemical, and mechanical properties of materials since these modeling approaches can track atom positions and forces. Such simulations provide a convenient way to investigate correlations between atomic-scale structure and the properties of molecular systems. Atomistic simulations can also complement experimental techniques to reduce the number of formulations that need to be tested and provide design guidelines. There are many different atomistic simulation methods

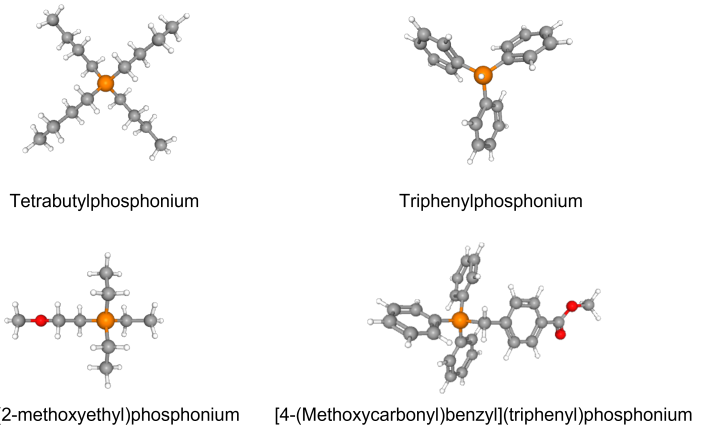

Fig. 1 Snapshots of atomistic models of representative phosphonium cations. Sphere colors correspond to atoms type: grey C, white H, red O, and orange P.

available [29], but here we focus on molecular dynamics (MD) simulations with empirical interatomic potentials, or force fields.

MD simulations are useful tools for studying ILs because they enable calculation of physico-chemical properties of the fluids at different temperature and stress conditions. More importantly, they provide information about atomic-scale mechanisms underlying observed properties and behaviors [30]. Such information can potentially be used to guide the selection or design of IL lubricants. This review will cover MD simulation-based studies of phosphonium ILs. Although the scope of the review is limited to phosphonium ILs, simulations of other ILs will be mentioned to provide context for observations and results, and to motivate future research directions. The review will include studies specifically focused on ILs as lubricants as well as studies designed for other applications that modeled material properties or interactions relevant to lubrication.

The review will begin with a brief introduction to MD simulation methods. This section will focus on the force fields/potentials used in the simulations since those are critical to the accuracy of results. The most widely used reactive and non-reactive force fields developed for studying phosphonium ILs properties will be introduced. Simulation analysis techniques focusing on cation-anion interactions, which play a determining role in physico-chemical properties of phosphonium ILs, will also be introduced. Next, we will review simulation predictions of physico-chemical properties of phosphonium ILs: density, viscosity, self-diffusivity, ionic conductivity, heat capacity, and thermal stability. Then, the effect of interactions between phosphonium ILs and other chemical species, particularly water and CO_2, on IL properties and behavior will be discussed, as well as wetting and confinement by solid surfaces. Lastly, based on the summary of previous work, opportunities for future MD simulation-based studies to understand and guide design of high-performance phosphonium ILs will be identified.

2 Molecular Dynamics Simulations of ILs

2.1 Empirical force fields

In MD simulations, the state of a given molecular structure and its temporal evolution are calculated by Newton's equations of motion [31]. In classical MD simulations, force is calculated from empirical equations that approximate the quantum-mechanical interactions between atoms, called force fields or potentials. The accuracy of MD simulations is highly dependent on the accuracy of the force field.

There are two broad categories of empirical potentials, reactive and non-reactive. Non-reactive potentials assume permanent covalent bonds between the atoms and cannot be used to study chemical reactions. However, non-reactive potentials are very efficient for predicting thermo-physical properties like density, viscosity, and heat capacity due to their simplicity and low computational cost. Hundreds or thousands of molecules, depending on their size, can be modeled for hundreds of nanoseconds using this approach. Reactive force fields, although less computationally efficient than non-reactive models, capture the formation and breaking of chemical bonds and so are suitable for modeling properties such as thermal stability as well as reactions between species. Here, the most widely used reactive and non-reactive force fields for studying phosphonium ILs are introduced.

The non-reactive force fields for ILs can be classified into two categories: polarizable [32–38] and non-polarizable [39–44]. Non-polarizable force fields handle individual atoms as point masses with fixed atomic charge, and do not explicitly consider the polarization of the atoms as a response to external electric fields, while polarizable force fields include explicit treatment of the polarization effect to improve the calculation of electrostatics [45].

Studies have shown that the polarizable force fields are better able to model the physico-chemical properties of ILs [32–38]. The polarizable force fields are more computationally expensive than their non-polarizable counterparts. However, the greater computational power now available to researchers has enabled polarizable force field-based simulations on time and length scales long enough to ensure proper sampling of the phase space. Unfortunately, there are still relatively few polarizable models for phosphonium ILs [32–38]. The Atomistic Polarizable Potential for Liquids, Electrolytes, & Polymers (APPLE&P) is currently the only polarizable force-field applied to study phosphonium ILs [33]. Therefore, parameters for non-polarizable force fields, such as AMBER [46] and OPLS [47], have been refined or revisited to better predict the interactions in ILs. IL-specific parameters have been developed for AMBER [48–50], the generalized Amber force field (GAFF)[51, 52], CLASS I (based on the AMBER framework) [53], DREIDING[35], OPLS [54, 55], and CL&P (based on the OPLS framework) [44, 56–60]. These optimized force fields have been shown to simulate the mechanics that dominate phosphonium IL properties on the molecular level with reasonable accuracy. Among these force fields, the AMBER force field parameter sets have been developed for the widest range of phosphonium ILs cation-anion pairs [8, 35, 48, 50, 61–65].

Since non-reactive force fields cannot capture bond dissociation and formation, they are not able to model some properties. This limitation is overcome by reactive force fields that have been developed to study various materials, systems, and chemical reactions [53]. Unfortunately, reactive force fields developed for ILs are even rarer than non-reactive force fields, due to the difficulty of the parameterization procedure and the extensive ab initio data sets for proper fitting of the numerous force field parameters [53]. The only reactive force field for which a parameter set has been developed specifically for ILs is ReaxFF [66]. An IL-specific ReaxFF parameter set was developed to study the chemical and physical interactions in a mixture of [P4,4,4,4][Gly]and CO_2 [67]. In this force field, polarization effects are considered through a geometry-dependent charge equilibration scheme. Further, a shielding term was included to avoid excessively close-range nonbonded interactions between the anions and cations. Since this is the only reactive potential available for ILs, there are just a few simulation studies of properties that involve chemical reactions of phosphonium ILs.

2.2 Simulation analysis methods

The interactions between ions have been widely used to understand and predict the physical properties of ILs [68, 69]. The three main types of interactions in neat ILs are cation-cation, cation-anion, and anion-anion. All three types of interactions may affect lubricant properties and can be analyzed using the methods described in this section. However, most previous studies have focused on cation-anion interactions to explain properties and trends [64, 70–72]. For ILs as additives or ILs with impurities, interactions with other chemical species also need to be considered. Interactions between ions, and between ions and other species, have been characterized by interionic/intermolecular interaction energies, radial distribution functions, spatial distribution functions, charge distributions, and hydrogen bonding [8, 64, 70, 71, 73].

First, the interaction energy of ion pairs plays a crucial role in determining the ionic dissociation/association dynamics of ILs [68]. Therefore, interionic interaction energies can be used to understand the physical properties of ILs [69, 74]. Interionic/intermolecular interaction energies are calculated from simulations as the sum of electrostatic and van der Waals interactions between atoms [62, 73].

A radial distribution function (RDF) quantifies the probability of finding an atom at some distance from a reference atom. It is obtained from simulations by calculating the distance between all atom pairs and binning them into a histogram [31]. A representative RDF for [Tf_2N] and six different phosphonium cations is shown in Figure 2. RDFs are important because they can be used to link microscopic details to macroscopic properties. Generally, a higher first peak in the cation-anion RDF indicates stronger interactions [62] while the position of the peak corresponds to the interaction distance [50].

One of the limitations of an RDF analysis is that detailed information of the local liquid structure can be lost due to cancellation of contributions from regions of low and high probability at the same distance but different parts of the local structure [75, 76]. Therefore, one-dimensional RDFs are unable to characterize uniquely the

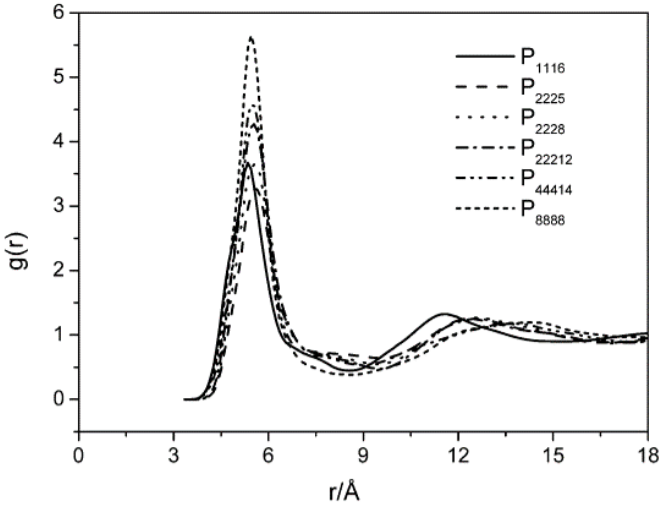

Fig. 2 Representative RDF between P_{cation}-N_{anion} in ILs with [Tf_2N] and six different phosphonium cations. The height and position of the first peak are used to quantify cation-anion interactions [62]. Figure reprinted with permission from J. Phys. Chem. B 2012, 116, 16, 4934–4942. Copyright 2012 American Chemical Society.

local spatial assembly of molecules (ions) in a liquid [76]. Spacial distribution function (SDF) analyses overcome the limitations of RDFs. Specifically, SDFs capture both the radial and angular coordinates of the interatomic separation vector. SDFs between all independent atomic pairs can provide the 3-dimensional neighborhood surrounding a molecule (ion) or atom in the local coordinate system [76, 77]. Representative SDFs for [P4,4,4,8] with four different anions are shown in Figure 3. Such analysis can provide information about the local structure in molecular liquids that is not available in a RDF.

Next, the charge distribution across an IL affects chemical and separation processes [78]. The charge distribution is recognized as an essential feature of ILs, influencing properties on the molecular as well as on the macroscopic scale.

Next, the charge distribution across an IL affects chemical and separation processes. The charge distribution is recognized as an essential feature of ILs, influencing properties on the molecular as well as on the macroscopic scale. For non-polarizable force fields, charge distributions are calculated from the electrostatic potential surrounding the molecule or fitted to reproduce experimentally measured condensed phase properties, while polarizable force fields specify charge distributions through an induced dipole or Drude oscillator. In reactive force fields, charge distributions are obtained using the charge equilibration method, which assumes that the system is a contiguous conductor and charge transfer can occur across any distance.

Lastly, hydrogen bonds (or H-bonds) are responsible for many of the physical and chemical properties of ILs, such as solubility, ionic conductivity, melting point,

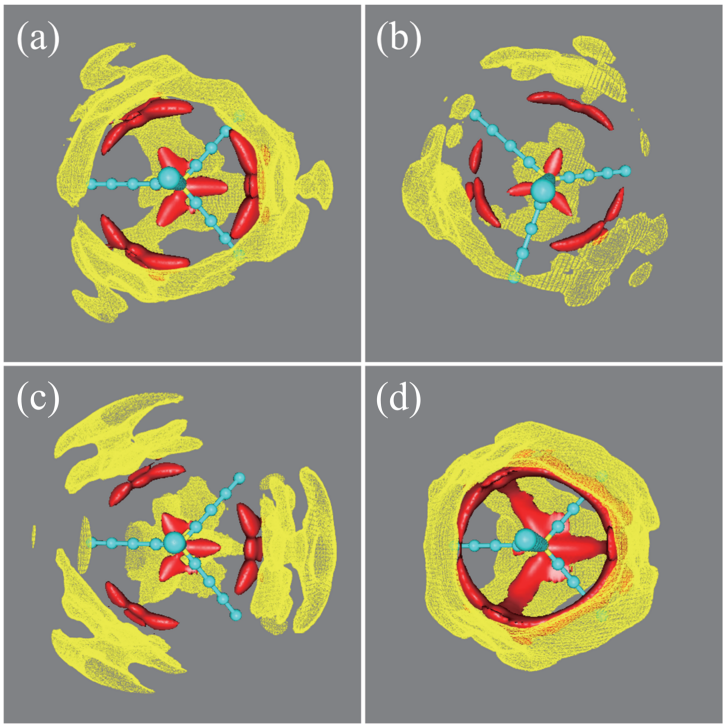

Fig. 3 Representative SDFs of the B atom (yellow meshed surface) and all O atoms (red solid surface) in (a) [BMB], (b) [BMLB], (c) [BOB], and (d) [BScB] anions around the [P4,4,4,8] cation (P and C atoms are represented by yellow and cyan beads, respectively) obtained from atomistic simulations. In each case, the red and yellow bounded contour surfaces are drawn at 5.5 and 4.0 times the average density, respectively [35]. Figure reprinted with permission from J. Phys. Chem. B 2014, 118, 29, 8711–8723. Copyright 2014 American Chemical Society.

viscosity, thermal stability, wettability, and vaporization enthalpy [79, 80]. Hydrogen bonds are identified in a simulation based on hydrogen-to-acceptor distance and acceptor-hydrogen donor angle [81], although the criterion for these two parameters may vary for different systems [50, 62].

These analysis methods have been used separately and in combination to explain observations and trends in physico-chemical properties, as discussed next.

3 Physico-Chemical IL Properties

In this section, the properties of phosphonium ILs and their relevance to lubricants will be introduced, along with a brief description of the methods used to calculate each property. Simulation-calculated values for each property will be summarized, in table form, with comparison to experimental data when available. When possible, the accuracy of values obtained with different force fields will be compared. Finally, trends with respect to temperature, interactions with other chemical species, and the anion and cation chemistries will be identified and analyzed.

3.1 Density

Density plays a role in how a lubricant functions because it affects fluid flow properties. Also, higher density increases the amount of time it takes for particles to settle out of suspension. As such, high-density fluids exhibit better contamination control by aiding in the suspension, transport, and removal of particulate contaminants [82]. Also, in some applications, density increases the erosive potential of the fluid [83].

Density is the most commonly reported property from MD simulations because it is relatively easy to calculate. Density is obtained from MD simulations at constant temperature and pressure [62]. During such simulations, the volume of the model system varies depending on the temperature and pressure conditions specified. Convergence of the simulations is determined based on the energy and volume reaching steady-state, i.e., fluctuating about a constant value [84]. Then, density is calculated from the volume averaged during steady-state divided by the total mass of atoms in the system [31].

A summary of densities calculated from MD simulations and comparison to experimental data are presented in Table 1. The phosphonium ILs in this and all subsequent tables are listed in order of anion type.

For density prediction of phosphonium ILs, the AMBER force field (including GAFF) is the most frequently used potential. The difference between simulation and experimental results for density is typically small (less than 3%) when using this potential. However, some simulations have a relative error of more than 4%, like those for [P1,1,1,6][Tf_2N] and [P4,4,4,4][Gln]. The larger error for [P1,1,1,6][Tf_2N] was attributed to the force field parameters for the carbon atoms bonded to the phosphorus atom [62]. It has also been reported that the accuracy of simulated densities using the AMBER force field could be improved by fine-tuning the interaction parameters [62]. Other potentials, including OPLS, CL&P, APPLE&P, DREIDING, and ReaxFF, have also been used to predict the density of phosphonium ILs. These other potentials predicted density with good accuracy (error less than 2%), although fewer phosphonium ILs have been studied using them compared to AMBER.

From Table 1, it can be seen that [P6,6,6,14][Cl] was modeled using OPLS, GAFF and CL&P, with OPLS and CL&P giving more accurate density than GAFF. This suggests that, if parameter sets are available, OPLS and CL&P force fields have higher accuracy for predicting density. Otherwise, the AMBER force field can be used since parameter sets have been developed for a wide range of cations and anions pairs for phosphonium ILs. Although ReaxFF was shown to predict density with reasonable accuracy for [P4,4,4,4][Gly], parameters have not been developed for many different ILs and this force field is less computationally efficient than non-reactive force fields, which limits the size of systems that can be modeled.

The densities reported in Table 1 were mostly calculated at a fixed temperature (usually room temperature) to validate the potential [35, 50, 62]. However, there are some studies that simulated the density of phosphonium ILs at different temperatures and showed density decreased with increasing temperature [51, 61, 89], as also observed in experimental studies [91–94]. This trend was explained by the fact that interactions between cations and anions become weaker with increasing temperature, as demonstrated by SDF analysis [61].

The presence of water was shown to decrease the density of [P1,1,1,1][Gly] and [P4,4,4,4][Gly] and the effect was attributed to strong interactions between hydrophilic glycinate and water that, in turn, weakened the interactions between the cation and glycinate [72]. It has also been found that chemical adsorption of CO_2 increased the density of five different [P4,4,4,4]-based ILs [85]. ReaxFF parameters were developed specifically to capture the physical and chemical interactions between [P4,4,4,4][Gly] and CO_2 [67]. The simulated reaction pathway for CO_2 and [Gly] anion is shown in Figure 4. The trained ReaxFF force field was then used to calculate the density with error less than 1%. The simulations also predicted a significant increase in density with increasing CO_2/IL ratio, larger than predicted by the non-reactive AMBER force field [50]. This larger increase from reactive MD simulations was attributed to bonding between CO_2 and the [Gly] anion, which reduced the volume and thus increased the density of the system [67].

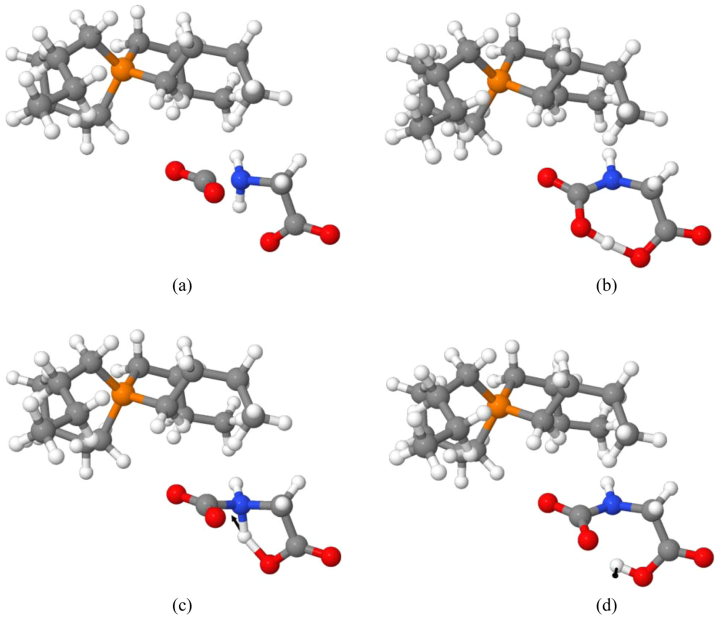

Fig. 4 Snapshots of [P4,4,4,4][Gly] and CO_2 at different steps in the reaction pathway obtained from a reactive MD simulation [67]. Sphere colors correspond to atoms type: grey C, white H, blue N, red O, and orange P. Figure reprinted with permission from J. Phys. Chem. B 2014, 118, 41, 12008–12016. Copyright 2014 American Chemical Society.

Table 1 shows that density depends on both cation and anion. First, it has been reported that density decreases with increasing cation size for the same anion [35, 95]. This trend is observed in Table 1 where density increases as [P8,8,8,8] < [P4,4,4,14] < [P2,2,2,12] < [P2,2,2,8] < [P2,2,2,5] < [P1,1,1,6] for [Tf_2N] anions. The same trend is observed for chelated orthoborate anions with density increasing as [P6,6,6,14] < [P4,4,4,14] < [P4,4,4,8]. It was proposed that longer cation alkyl chains increase the interionic separation and lower the packing efficiency, resulting

in more volume occupied by the cations and a lower overall density [35, 95, 96].This explanation was supported by an analysis that showed longer cation alkyl chains had lower interaction energies which led to less efficient packing of ions [35].

The anion can also affect density. For non-phosphonium ILs, some studies reported that density increased with the molecular weight of anions [97, 98]. This trend is observed for [P6,6,6,14]-based ILs in Table 1, where both density and molecular weight increase as [Cl] < [AcO] < [DCA] < [Br]. Further, for the difference between [DCA] and [Br], RDF peaks for [DCA] were found to be broader and less pronounced than those of [Br]. This trend was attributed to the anion structure. The spherical shape of [Br] had high charge-density, which allowed the ions to come closer to the [P6,6,6,14] cation, whereas the angular shape of [DCA] had a diffused charge distribution, hindered this process which led to a lower density [88].

However, other studies showed results that do not follow this trend [99] or even exhibited the opposite trend [100]. As observed in Table 1, for [P4,4,4,8] and [P4,4,4,14] cations, density increases as [BMB] < [BScB] < [BMLB] < [BOB], which is opposite to the trend in their anion mass. Similarly, for [P4,4,4,4] cations with amino acid anions in Table 1, density increases as [Leu] < [Ala] < [Gly] and [Phe] < [Met] < [Ser], exhibiting a trend inversely correlated to anion molar mass. The observation may be due to the greater number of carbon atoms in the heavier anions which increased occupied volume, following the same argument as proposed for cations with longer alkyl chains. Therefore, factors other than molar mass, such as atom type and polarity, also need to be considered to understand the effect of the anion on density.

3.2 Viscosity

Viscosity is a property of lubricants that quantifies a fluid's resistance to flow. Viscosity directly determines fluid film thickness and viscous friction and so is the dominant factor in tribological behavior, as well as mechanical efficiency in hydraulic applications. The rate of decrease of viscosity with temperature is particularly important because there is always frictional heating in a sliding contact. At a molecular level, viscosity is due to the interactions between and within molecules (ions) in a fluid. However, there have been fewer simulation studies of phosphonium IL viscosity than density because the simulations of viscosity are more complicated and time-consuming.

There are four main approaches to calculating viscosity in MD simulations. These methods are commonly known as Green-Kubo (GK), Einstein, direct non-equilibrium molecular dynamics (NEMD), and reverse non-equilibrium molecular dynamics (rNEMD) simulations [101]. The first two approaches are equilibrium molecular dynamics (EMD) simulation approaches whereas the last two are non-equilibrium molecular dynamics (NEMD) approaches. EMD approaches are used to calculate viscosity at low shear rates, i.e., Newtonian viscosity, while NEMD approaches are used to calculate viscosity at high shear rates. However, low shear viscosity can be estimated from the NEMD approaches by fitting the high shear rate viscosity data to an empirical equation, such as the Carreau or Eyring equation, and extrapolating back to low shear rates [64, 102, 103].

Both the GK and Einstein approaches calculate low shear viscosity as a function of simulation box volume, Boltzmann constant, temperature, time, and stress. The difference between them is that the GK approach relates the ensemble average of the autocorrelation of stress to viscosity, [64, 89] whereas the Einstein approach relates the ensemble average of the mean-square displacement (MSD) of the stress tensor to viscosity [33]. Of the two EMD approaches, GK is more widely used since it is easy to implement and has been reported to accurately predict viscosity when viscosity is relatively low [64, 104]. However, the autocorrelation functions of stress take a long time to converge, especially when the viscosity of the liquids is over 20 mPa·s [105]. In such cases, the Einstein approach is a more computationally efficient and reasonably accurate approach [106, 107].

In NEMD, shear flow simulations are performed by applying the SLLOD equations of motion [108]. The viscosity under high shear rate is obtained as the ratio of the shear stress and the velocity gradient [64]. NEMD was used to model [P6,6,6,14][Im] and [P6,6,6,14][ImC] to compare viscosity before and after CO_2 absorption and showed accuracy less than 20% even for high viscosity [109]. NEMD was also used for [P6,6,6,14][Cl] and [P6,6,6,14][BMB] to cross-check the viscosity results obtained from the GK relation [64]. However, most previous viscosity simulations for phosphonium ILs have used EMD methods.

A summary of Newtonian viscosities calculated from MD simulations and comparison to experimental data is presented in Table 2. In terms of simulation methods, the relative error of viscosity calculated from GK theory varies from around 7% to more than 50% for both [P6,6,6,14][Cl] and [P6,6,6,14][BMB] at different temperatures and has 8% error for [P2,2,2,2O1][Tf_2N] at 400 K. With the Einstein relation, viscosity calculations for [P2,2,2,5][Tf_2N] at temperatures of 298 K and 373 K showed good agreement with experimental data, with error less than 10%. However, the error increased to around 20% for [P2,2,2,8][Tf_2N] at 373 K and more than 60% for [P6,6,6,14][Tf_2N] at 293 K. Overall, the GK and Einstein relations give similar accuracy for phosphonium IL viscosity.

As expected, the accuracy of all EMD calculation methods is lower for higher viscosity ILs in Table 2. Therefore, equilibrium methods for calculating viscosity are best for modeling phosphonium ILs with low viscosity as well as blends of phosphonium ILs with base oil, whose viscosity is usually much lower than neat ILs.

From Table 2, it can be seen that the APPLE&P (polarizable), AMBER, OPLS, and OPLS-based CL&P force fields have been used to simulate viscosity of phosphonium ILs. APPLE&P exhibited good agreement with experimental study, even though the viscosity is over 20 mPa·*s*. However, only [P2,2,2,5][Tf_2N] has been studied using this potential. The AMBER, OPLS, and CL&P force fields have been used more frequently. However, their overall accuracy, which decreases as viscosity increases, is lower than that for APPLE&P for [P2,2,2,5][Tf_2N]. This is consistent with previous studies that reported polarizable force fields are better able to model the physico-chemical properties of ILs [33–38].

Like density, some studies only calculated the viscosity of phosphonium ILs at a specific temperature. However, there are a few studies that simulated the

change of viscosity with temperature. For example, Table 2 reports the viscosity of [P6,6,6,14][Tf_2N] from 273 to 573 K, [P6,6,6,14][Cl] from 323 to 463 K and [$HP(Oct)_3$][TFO] from 393 to 465 K. Consistent with physical observations, MD simulations predict the viscosities of these phosphonium ILs decrease rapidly with increasing temperature. This trend was also reflected in an RDF analysis for [P6,6,6,14][Tf_2N] where the height of the first peak of H_{cation}-O_{anion}s RDFs decreased with temperature, indicating that interactions between cation and anion became weaker with increasing temperature, therefore contributing to lower viscosity [61].

It has been reported that chemical adsorption of CO_2 decreased the viscosity of [P6,6,6,14][Im]. This was explained by RDFs and SDFs that showed the anions became asymmetric after reaction with CO_2, which weakened the interaction between the phosphorus atom and the nitrogen atom of the anion. This weakened interaction led to faster dissociation of cation-anion pairs, thereby accelerating dynamics and lowering viscosity [109].

For the effect of cation on viscosity, it has been reported that higher symmetry or longer alkyl moieties in the cation generally lead to higher viscosity for a given anion [111–113]. This is seen in Table 2 where viscosity increases as [P2,2,2,5][Tf_2N] < [P2,2,2,8][Tf_2N] < [P2,2,2,12][Tf_2N] at 373 K and [P2,2,2,2][PhO] < [P3,3,3,3][PhO] < [P4,4,4,4][PhO] < [P6,6,6,6][PhO] < [P8,8,8,8][PhO] at 420 K. However, there are some exceptions; for example, [P6,6,6,6][PhO] and [P8,8,8,8][PhO] at 298 K. Table 2 also shows that, for the [Tf_2N] anion, viscosity is lower for [P2,2,2,2O1] than [P2,2,2,5], consistent with a previous report that the presence of alkyl ether chains decreases viscosity compared to alkyl chains [71].

For [P2,2,2,5], [P2,2,2,8], and [P2,2,2,12] paired with [Tf_2N], the effect of cation chain length on viscosity was analyzed using interionic interaction energy, RDFs for P_{cation}-N_{anion} and H_{cation}-O_{anion}, and hydrogen bonding [62]. It was found that the viscosity and interaction energy exhibited the same trend which suggested that the relatively high viscosities of ILs may due to the strong interactions between ions, consistent with a previous study that showed higher interionic interaction energy is correlated to higher viscosity for [EMIM]-based ILs [74]. Coordination numbers calculated by integrating RDFs showed that cations with shorter alkyl chain lengths were likely to be surrounded by more anions and molecule flowability increased as a result, leading to a lower viscosity. Lastly, stronger hydrogen bonding usually correlates to higher viscosity for different anions paired with the same cation [50, 114].

In a study of halogen-free chelated orthoborate-phosphonium ILs, the P_{cation}-B_{anion} RDFs for cations with longer alkyl chains exhibited a higher first peak and lower first minimum for the same anion [35]. This is in agreement with the trend that cations with larger alkyl groups have higher viscosity. In another study, the viscosity of [P2,2,2,5][Tf_2N] was found to be nearly twice that of [P2,2,2,2O1][Tf_2N] [72]. This was correlated to the P_{cation}-N_{anion} RDFs for which [P2,2,2,5][Tf_2N] had a higher first peak [71]. RDFs of P_{cation}-$C\alpha_{anion}$ for [P1,1,1,1][Gly] and [P4,4,4,4][Gly] showed that the first peak was higher but at a longer distance for [P4,4,4,4][Gly]. This

was believed to be caused by longer alkyl chains in the cations, which had stronger interactions with the anion even at a farther distance [72].

For the effect of anions, it has been reported earlier that viscosity increases with number of hydrogen bonds, as observed for structurally similar anions paired with [P4,4,4,4] where the viscosity increased as [Gln] > [Glu] > [Lys] > [Ser] [50]. From Table 2, at room temperature, tetraalkylphosphonium (like [P2,2,2,2]) ILs with [PhO] anion have very low viscosity (about 2 mPa·s), while tetraalkylphosphonium ILs with other anions (like [Cl], [BMB], and [Tf_2N]) have a viscosity over 75 mPa·s. Another observation from Table 2 is that viscosity increases as [P6,6,6,14][BMB] < [P6,6,6,14][Cl] < [P6,6,6,14][Tf_2N] at around 373 K. However, this trend is inconsistent with experimental data that showed the viscosity of [P6,6,6,14][Tf_2N] is lower than that of [P6,6,6,14][Cl] [11, 115] at 298 K, indicating temperature also affecting viscosity trends. Further, these anions have significant structural differences that are likely to affect the viscosity more than hydrogen bonding. Therefore, additional simulation works should be carried out, ideally with anions for which the key difference is hydrogen bonding, to confirm the trends.

3.3 Self-diffusivity

Self-diffusivity describes the rate of net movement of molecules from a higher concentration region to a lower concentration region. This property is quantified by the self-diffusion coefficient. Te self-diffusion coefficient has been found to be proportional to temperature and inversely proportional to viscosity [33]. Self-diffusivity has been studied in MD simulations for phosphonium ILs to evaluate the ability of a given force field to predict transport properties or to explain observed trends [33, 35].

In MD simulations, the self-diffusion coefficient is usually calculated using the Einstein relation based on the mean-square displacement (MSD) of the center-of-mass of the ions [33, 35, 52, 116]. It can also be calculated by the time integral of the velocity autocorrelation function using the GK expression [55]. However, self-diffusion coefficients calculated using GK are typically higher than those obtained from the Einstein relation [55]. The self-diffusion coefficient is calculated separately for the cation and anion.

A summary of self-diffusion coefficients of phosphonium ILs from MD simulation is presented in Table 3. There are very few experimentally measured self-diffusion coefficients reported that can be used to evaluate the accuracy of model predictions, so error is not reported in Table 3. However, reference data is available for [P2,2,2,2O1][Tf_2N] [65]. For this IL, the self-diffusion coefficient was calculated using the AMBER force field to be 450×10^{-12} m^2/s for the anion and 410×10^{-12} m^2/s for the cation. These are larger than the experimental values of 340×10^{-12} m^2/s for the anion and 290×10^{-12} m^2/s for the cation [65].

For the influence of temperature, the self-diffusion coefficients of both cation and anion in phosphonium ILs increase with temperature, as observed for ILs like [P6,6,6,14][Tf_2N] and [P4,4,4,4][2-CNpyr] in Table 3. Further, the rate of increase of self-diffusion coefficient with temperature is faster at higher temperatures [51, 52, 61].

Self-diffusion and viscosity are inversely related [33]. In Table 3, for [P4,4,4,8] and [P4,4,4,14] cations, the self-diffusion coefficient is larger for [BScB] than [BMB]. The self-diffusion coefficients of these ILs exhibit the opposite trend with the viscosity of [BMB] larger than [BScB] [17]. The same inverse relationship is observed for [P6,6,6,14] ILs, for which the self-diffusion coefficients increase as [BOB] < [BMLB] < [BMB] < [BScB], while viscosity exhibits the opposite trend [17]. These results confirm that self-diffusion coefficient phosphonium ILs are generally inversely proportional to viscosity.

The presence of water is expected to increase self-diffusivity because the addition of water decreases counterion association, thereby allowing ions to diffuse more freely. For example, the self-diffusion coefficients of both the cation and anion increased when water was present in [P2,2,2,8][2-CNpyr] and [P2,2,2,8][3-Triaz] systems, with the anions exhibiting a larger increase [117]. The same trends were observed in an earlier study with [P4,4,4,4][2-CNpyr] and [P4,4,4,4][BnIm] ILs [85]. However, for ions with low self-diffusivity, the effect of water can be negligible. For example, the ions in [P1,1,1,1][Gly] and [P4,4,4,4][Gly] had similar self-diffusion coefficients in neat form and with 10% water [72].

The self-diffusion coefficients of ions were compared to that of water for [P4,4,4,4][2-CNpyr] and [P4,4,4,4][BnIm] ILs [85], and [P1,1,1,1][Gly] and [P4,4,4,4][Gly] [72]. In all cases, water diffused much faster than either ion. This is consistent with the fact that the ions are much larger than the water molecules [85]. Further, for [P4,4,4,4][2-CNpyr] and [P4,4,4,4][BnIm], the self-diffusion coefficient for water in [P4,4,4,4][2-CNpyr] was higher because of the hydrophobicity of the IL. Although hydrogen bond formation was found between water and the anions, cation–anion center-of-mass RDFs showed that the water did not affect the overall structure of the ILs [85].

As seen in Table 3, the self-diffusion coefficients of cations and anions are not the same for a given IL and that most anions have higher diffusion coefficients than cations in phosphonium ILs. It has been proposed that this is due to the fact that anions do not have long alkyl chains and occupy a smaller volume, so they experience less steric hindrance and are able to move more easily than cations [52], suggesting that the shape of the ions plays an important role [85]. The only outlier in Table 3 is [P6,6,6,14][Tf_2N], where [P6,6,6,14] has a higher diffusion coefficient than [Tf_2N] at 398 K. This is due to the fact that the self-diffusion coefficient increased faster with temperature for the [P6,6,6,14] cation than the [Tf_2N] anion [52].

For the cations, self-diffusion coefficients are smaller for longer alkyl chains. For example, the self-diffusion coefficient decreases as [P2,2,2,5] > [P6,6,6,14] for the [Tf_2N] anion, [P2,2,2,8] > [P4,4,4,4] for the [2-CNpyr] anion, and [P2,2,2,2] > [P3,3,3,3] > [P4,4,4,4] > [P6,6,6,6] > [P8,8,8,8] for the [PhO] anion. This is consistent with the observed increase of viscosity with cation alkyl chain length, since self-diffusion coefficients and viscosity are inversely related [57, 61]. Therefore, the self-diffusion trends for cations may be explained using the same mechanisms as proposed for viscosity.

There is no consistent trend observed for the anions in Table 3. For example, the self-diffusion coefficient increases as [BMLB] < [BMB] < [BScB] < [BOB] for

[P4,4,4,8] and [P4,4,4,14] cations, but the trend is [BOB] < [BMLB] < [BMB] < [BScB] for the [P6,6,6,14] cation. It is also observed that, for the [P2,2,2,8], the self-diffusion coefficient increases as [3Triaz] < [PhO] < [2-CNpyr]. However, there is no clear explanation for this trend.

3.4 Ionic Conductivity

Ionic conductivity is a measure of the IL's ability to conduct electricity. Ionic conductivity is important for lubricants that operate in the presence of electric contact [118]. For example, in electric motors, rolling bearings and their lubricants are subjected to stray current, which can lead to bearing damage. Usually, lubricants with moderate ionic conductivity are preferred to minimize static charge while also avoiding short-circuiting of lubricated contacts [119, 120].

There are various EMD simulation approaches for calculating ionic conductivity of a material, including GK, Einstein, and Nernst-Einstein. Like viscosity and thermal conductivity, the GK formula relates the time integral of the autocorrelation of electric current to the ionic conductivity [89, 121] whereas the Einstein equation relates the mean square displacement of electric current [33, 121, 122]. The Nernst-Einstein equation is a more computationally efficient approach that relates the the self-diffusion coefficient of anions and cations and their charges to ionic conductivity [122, 123] if translation of counterions is excluded from the calculated diffusion coefficient [122].

A summary of the ionic conductivity of phosphonium-based ILs from MD simulation is presented in Table 4. Currently, there are only two previous studies that compared ionic conductivity between MD simulations and experiments. For [P2,2,2,5][Tf_2N], the difference between experiment and simulation was reported to be 23% [33], and for [P2,2,2,2O1][Tf_2N] it was around 40% [65]. Generally, the conductivity of ILs increases with temperature [61, 89] since temperature increases the mobility of the ions. This trend can be seen for the ILs in Table 4.

From the Einstein relation, ionic conductivity is proportional to self-diffusivity and inversely proportional to viscosity [57, 61]. This relationship can be seen by comparing the ionic conductivity in Table 4 and the viscosity in Table 2 for [P2,2,2,5][Tf_2N] and [P2,2,2,2O1][Tf_2N]. The high ionic conductivity and lower viscosity of [P2,2,2,2O1][Tf_2N] was attributed to the higher ionic mobility of the alkyl ether chain in the [P2,2,2,2O1] compared to the alkyl chain in the [P2,2,2,5] [71]. It was also found the addition of [Li] cation decreased ionic conductivity and increased viscosity for [P2,2,2,2O1][Tf_2N] [71]. Both trends are attributable to the strong interactions between the metallic cation and the [Tf_2N] anion.

For the effect of cation, it is observed in Table 4 that ionic conductivity decreases with cation alkyl chain length as [P2,2,2,5] > [P2,2,2,8] > [P2,2,2,12] with [Tf_2N]. The higher viscosity of ILs with longer cation alkyl chains have higher viscosity which hinders ionic mobility leading to lower ionic conductivity. For the effect of anions, currently there are too few MD simulation studies to identify trends. Future studies may analyze trends among anions in terms of previously reported correlations between ionic conductivity and both interionic interaction energy [68] and hydrogen bonding [50, 80].

3.5 Heat capacity

Heat capacity is a measure of the amount of heat energy required for a unit change in temperature. Usually, higher heat capacity helps a lubricating oil to carry heat away from a sliding interface, thereby extending the life of mechanical parts. In MD simulations, constant-pressure heat capacity is calculated from the rate of change of the enthalpy of the system with temperature [50, 61, 124].

A summary of the heat capacities of phosphonium ILs from MD simulations with comparisons to experimental data is presented in Table 5. Currently, only the AMBER and GAFF force fields have been used to calculate heat capacity for phosphonium ILs. GAFF was used to calculate the heat capacity of [P4,4,4,4][2-CNpyr], but there is no experimental data available to evaluate the accuracy of the predictions. The AMBER force field was used to calculate the heat capacity of [P4,4,4,4]-based ILs, with relative error ranging from 1% to 12% for most anions, but 18% error for [Gly] and more than 40% error for [Lys]. However, for [P4,4,4,4][Lys], another experimental study [125] reported heat capacity much closer to the simulation-calculated value, leading to error of less than 5%.

The heat capacity of phosphonium ILs has been reported to increase with temperature from experimental studies [94, 126, 127], but no MD simulation studies have investigated trend. Chemical adsorption of CO_2 has been shown to increase the heat capacity of [P4,4,4,4][2-CNpyr] [51]. The increase in heat capacity was attributed to the ions being slightly farther apart with little change to the nonbonded van der Waals and electrostatic interactions. This caused the [P4,4,4,4][2-CNpyr-CO_2] to require more heat to increase temperature than the unreacted system [51].

For the effect of the cation, the results in Table 5 show that the heat capacities of [P4,4,4,4]-based ILs are higher than those of [P6,6,6,14]-based ILs, suggesting that heat capacity decreases with increasing cation alkyl chain length. However, additional simulations should be carried out to confirm the trend for other anions. In Table 5, the heat capacity for [P4,4,4,4] cations increases as [Glu] < [Asp] < [Leu] < [Ala], which is opposite to the anion mass trend [50]. This trend too could be investigated with future simulations of ILs with similar anion structures.

3.6 Water Solubility

Water is widely used during IL synthesis [128–131], and many ILs have high water affinity. Consequently, it can be difficult to remove water from a produced IL which can then significantly affect properties including density, viscosity, polarity, conductivity, and solubility [79, 85, 94, 117]. The solubility of ILs in water is also very important for reducing emulsification when preparing water-based lubricants [132].

The water solubility of five different [P4,4,4,4]-based ILs was compared based on the solvation free energy of water going from an ideal gas state to dissolved in IL. It was found that [2-CNpyr] had the lowest water solubility, while [BnIm] had highest water solubility [85]. Another study compared the solubility of ILs with [P4,4,4,4] cation and three different anions [73]. Results showed that [P4,4,4,4][CF_3COO] was completely miscible with water, [P4,4,4,4][CF_3COO]-H_2O was partially miscible with water, and [P4,4,4,4][PF_6] was not soluble in water. Analysis showed that

cation-anion and anion-H_2O interactions were primarily electrostatic, while van der Waals interactions were dominant for cation-H_2O [73].

MD simulations were used to study the mixing behavior between water and phosphonium ILs with chloride and acetate anions. While the anions were well solvated with water due to their small size, only the smallest cation [P2,2,2,2] was completely miscible with water forming a homogeneous binary solution. As the length of cation alkyl chain increased, the size of heterogeneous domains increased and ultimately led to stable interfaces between water and ILs [87]. Chemical reaction with CO_2 has been found to increase water solubility of [P4,4,4,4]-based ILs. Among several ILs studied, the increase of water solubility due to CO_2 was largest for the [2-CNpyr] anion [85].

Hydrogen bond analysis has been widely used to study interactions between ions and H_2O. Particularly, hydrogen bonding between water and anions can weaken the interactions between cations and anions [73, 133]. This relationship is shown in Figure 5 for [P6,6,6,14][BOB] where the effect of water is observed to be highly dependent on water concentration. This dependence was attributed to the competition between hydrogen-bond interactions, electrostatic interactions between the polar segments in the ionic species, and dispersion interactions between the hydrophobic alkyl chains in the cations [133]. Simulations of [P6,6,6,14]-orthoborate in water showed that, even after the bulk water was removed, some water molecules were trapped between the adjacent ionic species [63]. The number of hydrogen bonds between the ILs and water molecules was found to decrease rapidly with increasing temperature for [P4,4,4,4] paired with [CF_3COO], [CH_3COO], and [PF_6] [73].

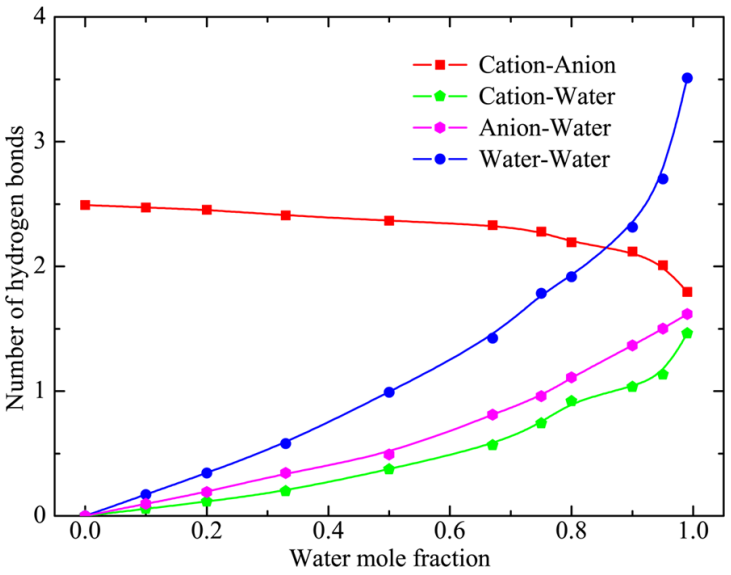

Fig. 5 Number of hydrogen bonds in the cation-anion, cation-water, anion-water, and water-water pairs calculated from the [P6,6,6,14][BOB] IL/water mixtures as a function of water mole fraction [133]. Figure reprinted with permission from J. Phys. Chem. B 2015, 119, 16, 5251–5264. Copyright 2015 American Chemical Society.

3.7 Thermal stability

The thermal stability of phosphonium ILs is important for their application as lubricants because chemical decomposition causes lubrication performance decreasing over time. Although there are quantum chemistry simulations and ab initio MD simulations studying thermal degradation of phosphonium ILs [134–137], classical MD simulation studies using an empirical force field are very limited. This is largely because thermal decomposition involves bond dissociation which cannot be modeled using non-reactive simulations.

An alternative simulation approach is reactive MD that can capture chemical reactions [138, 139]. Especially, reactive MD simulations using ReaxFF [66] have been used to investigate thermal decomposition of various chemical species, including hydrocarbon fuels [140–142], polymers [143], insulation gas [144], refrigerants [145, 146], energetic materials [147, 148], and phosphate-based lubricant additives [149, 150]. One ReaxFF parameter set has been developed specifically for a phosphonium IL [67].

In a recent study, ReaxFF simulations with this parameter set were used to compare thermal decomposition of [Benz] and [Sali] anions with three phosphonium cations [151]. Simulation results and experimental measurements showed that the [Benz] ILs were less thermally stable than the [Sali] ILs, but there was little effect of the cation. Then, the simulations were used to isolate decomposition reaction pathways, one of which is shown for [P4,4,4,4] [Sali] in Figure 6. It was found that the hydroxyl groups in the [Sali] hindered proton transfer, thereby decreasing the likelihood of subsequent decomposition reactions [151].

3.8 Interactions with Solid Surfaces

The MD simulation studies reviewed so far have focused on predicting and understanding the physico-chemical properties of bulk phosphonium ILs. However, lubricating fluids are often interacting with solid surfaces and confined to very narrow gaps between those surfaces during operation. This confinement can affect their material properties and also directly relates to tribological parameters such as friction and wear. Several previous studies have explored the frictional behavior of confined ammonium and imidazolium ILs [152–156].

One MD simulation study investigated the wetting of [P2,2,2,5][Tf_2N] on face-centered cubic platinum surfaces [157]. They found that contact angle was smaller on (111) orientated surfaces than (100) surfaces, as shown in Fig 7. Regardless, the contact angle was much lower than 90°on both surfaces, indicating [P2,2,2,5][Tf_2N] exhibited favorable wettability and hydrophilicity.

Simulations of phosphonium ILs confined to nanoscale gaps have also been performed, although not specifically related to lubrication. One study investigated the structure and capacitive behavior of phosphonium ILs confined between planar and porous graphene electrodes, as shown in Fig 8. It was found that the [P2,2,2,2O1][Tf_2N] ILs formed layers adjacent to the planar graphite electrodes but this ordering was disrupted by confinement between narrow nanoporous electrodes. Further, the differential capacitance on the negative electrode was lower than on

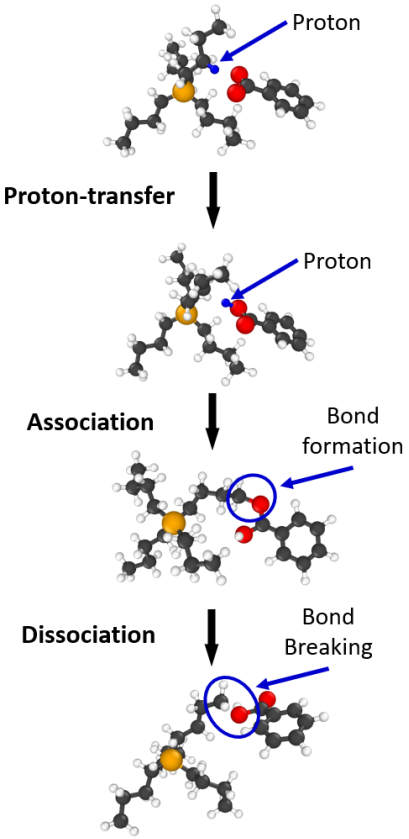

Fig. 6 Representative thermal decomposition pathway for [P4,4,4,4] [Sali] obtained from reactive MD simulations [151]. Sphere colors correspond to atoms type: black C, white H, red O, and orange P.

the positive electrode, which was attributed to the larger size of the [P2,2,2,2O1] cations relative to the [Tf_2N] anions that prevented efficient packing [65]. In another study, the interfacial ionic structure, molecular arrangement, and orientation of [P6,6,6,14][BMB] confined between neutral and charged gold electrodes was investigated. For both neutral and charged electrodes, the hexyl and tetradecyl chains in [P6,6,6,14] cations laid preferentially flat on the surface due to their elongated molecular conformation. In contrast, the [BMB] anions exhibited alternating parallel-perpendicular orientations adjacent to the neutral electrodes and gradually reached a parallel coordination pattern at the positively charged electrodes [158].

4 Summary and Future Research Opportunities

4.1 Review summary

This paper reviewed MD simulation studies of phosphonium ILs with emphasis on properties relevant to the use of ILs as lubricants. Previous simulations have

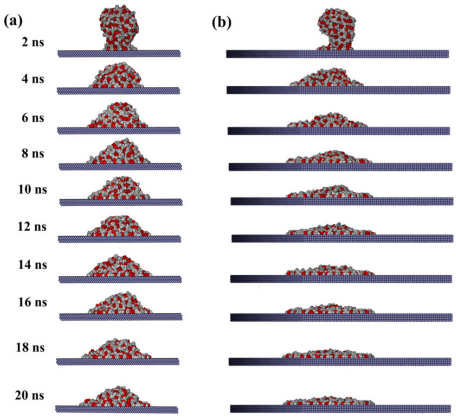

Fig. 7 Dynamic spreading of a [P2,2,2,5][Tf_2N] IL nanodroplet on (a) Pt(100) and (b) Pt(111) surfaces [65]. Sphere colors correspond to items type: white [P2,2,2,5]; red [Tf_2N]; ice blue Pt. Figure reprinted with permission from J. Phys. Chem. B 2020, 124, 14, 2835–2847. Copyright 2020 American Chemical Society.

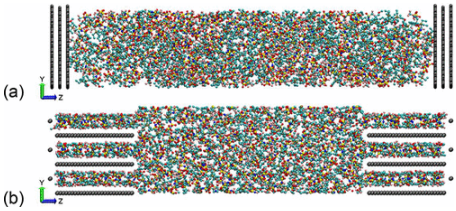

Fig. 8 Snapshots of simulations of [P2,2,2,2O1][Tf_2N] confined between (a) planar and (b) porous electrodes [65]. Sphere colors correspond to items type: black electrodes; other colors [P2,2,2,2O1][Tf_2N] ILs. Figure reprinted with permission from J. Phys. Chem. C 2019, 123, 17, 10816–10825. Copyright 2019 American Chemical Society.

used both non-reactive and reactive force fields, including AMBER, GAFF, OPLS, DREIDING, CL&P, APPLE&P, and ReaxFF.

The most frequently reported property is density and the simulation process is relatively simple and not time consuming. Density is often used as a first evaluation of the accuracy of a force field. The AMBER force field has been used most often and shown to predict density with error less than 3% for most ILs. However, for [P6,6,6,14][Cl], a comparison of multiple force fields showed that OPLS and CL&P were more accurate. Density was found to decrease due to the presence of water but increase when ILs chemically react with CO_2. An analysis of results for various ILs showed that density decreased with increasing cation size. This trend was attributed to higher interionic separation, quantified by interionic interaction energies and the position of the first cation-anion RDF peak, leading to lower packing density. A similar trend was observed for some anions where density decreased with increasing anion molar mass. But this trend was not always found, suggesting factors other than ion size are likely contributing. Generally, MD simulations can successfully predict density for phosphonium ILs and explain the effect of the cation. However, additional studies are needed to understand the effect of the anion on density.

Simulations have also been widely used to study the viscosity, perhaps the most important property of lubricating fluids. Although both equilibrium and non-equilibrium simulation methods are available for calculating viscosity, at this point, equilibrium simulations with the Green-Kubo method have been most often used to model phosphonium ILs. The error of viscosity calculated is higher than that reported for density, with error commonly above 10%. Also, the error of viscosity predictions is consistently higher for more viscous fluids. Force fields used for viscosity calculation are APPLE&P, AMBER, OPLS, and CL&P. A comparison of predictions for [P2,2,2,5][Tf_2N] showed that the most accurate was APPLE&P, although this force field has been used less frequently than the others because APPLE&P force field parameters have only been developed for a small number of anions and cations.

Simulations showed that viscosity decreases with increasing temperature and the trend was explained by cation-anion RDFs and SDFs, where the height of the first peak decreased with increasing temperature, indicating weaker interactions between anion-cation. Unlike density, increasing cation chain length was generally found to increase viscosity for the same anion. This was explained by RDFs that showed stronger interactions between cation and anion, i.e., higher first RDF peak, albeit at a further distance. In terms of the effect of anion, there is some evidence that viscosity was affected by anion size. However, anion shape was also shown to be important; spherical anions were able to get closer to the cation, leading to higher viscosity, while the opposite was observed for angular shapes.

Self-diffusivity has been calculated from many simulations, primarily as a means of understanding trends in transport properties. This property is not readily measured experimentally, so accuracy cannot typically be evaluated. However, for [P2,2,2,2O1][Tf_2N], the AMBER force field was shown to over-predict self-diffusivity for both cation and anion. Generally, the self-diffusion coefficient has been reported to be higher for anions than cations and the trend was attributed to the small occupied volume of the anions which enabled them to move more easily. For cations, self-diffusion coefficient was smaller for longer alkyl chains, opposite the trend of viscosity, as expected since these two properties are inversely related. There was no consistent trend observed for the anions. Lastly, it was shown that the self-diffusion coefficient usually increased in the presence of water because water molecules decrease counterion association such that ions can diffuse more freely.

Ionic conductivity has been calculated from a few simulation studies. Ionic conductivity was reported to increase with increasing temperature and decrease with increasing cation alkyl chain length, consistent with the trend for self-diffusion coefficient and opposite to that of viscosity. No consistent trend was observed for the anions. It has been suggested that higher ionic conductivity trends may be due to weaker hydrogen bonding.

Simulations have also been used to study heat capacity of selected phosphonium ILs using AMBER force fields. Some comparisons to experimental data have been performed and showed that the error ranges from 1% to tens of percent, depending on the IL. Although the relatively few number of studies performed precludes confirmation of trends, comparison of reported results suggested that heat capacities

are higher for cations with longer alkyl chain lengths, consistent with the trend in viscosity. Lastly, it was shown that adsorption of CO_2 increases heat capacity.

The solubility of ILs and water has also been studied and found to depend on both the cation and anion. Smaller anions were more soluble in water than cations, with larger cations being the least soluble. Chemical reaction with CO_2 has been found to increase the water solubility of ILs. Interactions between water and ILs was primarily analyzed in terms of hydrogen bonding and the competition between hydrogen bond interactions, electrostatic interactions between the polar segments of the anions, and dispersion interactions between the hydrophobic alkyl chains in the cations.

Thermal degradation occurs through bond dissociation and so can be studied only using reactive force field. The availability of only one reactive force field has therefore limited such studies. However, a recent study [151] compared the thermal stability of phosphonium ILs with three different cations and two different anions. It was reported that size and branching on the cation had little effect on thermal decomposition temperature but that even subtle chemical differences between anions could affect decomposition reaction pathways and therefore the thermal stability.

Lastly, a few studies have used models of ILs confined between solid walls to explore confined fluid behavior. The limited examples of that involved phosphonium ILs showed that the ions exhibit ordering near the walls and this ordering is affected by the porosity and charge of the solids.

4.2 Opportunities for future research

Although there have been many MD simulation studies focusing on phosphonium ILs, there are still many opportunities for future research in this area.

First, as mentioned in the context of multiple properties of phosphonium ILs, the effect of the anion is neither well characterized nor understood. Attempts to identify trends primarily focused on anion size, based on the observation that cation size effects are typically monotonic. However, the same trends are not always observed. Some studies suggested anion shape is likely to be important, but it is likely that multiple factors contribute to the effect of the anion on a given property. As seen in the reactive simulation study of thermal decomposition, even minor differences in the chemical nature of the anion can affect behavior of phosphonium ILs. Since anion chemistry and structure can be varied systematically in a simulation, this is a suitable tool for understanding the important role of the anion.

Viscosity is perhaps the most important property of a lubricant and studies using EMD simulations have characterized Newtonian, low-shear, viscosity for phosphonium ILs. High-shear viscosity is also important since lubricants can experience very high shear rates in thin lubricating gaps during operation. However, currently there few studies have calculated high-shear viscosity of phosphonium ILs using NEMD. Therefore, there are opportunities to use simulations to explore this important behavior. NEMD simulations could also be used to study viscous friction for phosphonium ILs.

Viscosity of phosphonium ILs has been simulated at different temperatures. However, the effect of pressure has not been investigated. The increase of viscosity with

pressure is quantified by the pressure–viscosity coefficient and is an important property of lubricants, particularly for elastohydrodynamic lubrication. EMD or NEMD simulations could be performed at different pressures to quantify and understand the origin of pressure-viscosity behavior for phosphonium ILs.

Thermal conductivity, the ability of a material to conduct heat, is very important for phosphonium IL lubricants because it determines how efficiently they can dissipate heat generated by the shearing of moving mechanical parts. Like viscosity, thermal conductivity of liquids can be calculated using EMD simulations with the GK method and NEMD simulations [159, 160]. EMD methods of calculating thermal conductivity have been applied to characterize ionic compounds like NaCl, MgO, Mg_2SiO_4 [161] and molten alkali fluorides [162]. However, these methods have not yet been applied to phosphonium ILs.

The thermal expansion coefficient quantifies the degree to which density changes with temperature at constant pressure. This property is important for storing or transportation of lubricants at different temperatures when the system may be heated to prevent lubricant overflow [163]. In MD simulations, the thermal expansion coefficient is estimated from a series of simulations at constant pressure but different temperatures as a linear fit of volume change with temperature [164]. It can also be calculated by taking the ensemble average of the fluctuations in volume and enthalpy that occur during an NPT simulation [164]. The thermal expansion coefficient of imidazolium-based ILs has been calculated in MD simulations and the results correlated well with experiment [165, 166]. However, there are only a few experimental measurements of the thermal expansion coefficient for phosphonium ILs [94, 167, 168] and MD simulation studies on phosphonium ILs thermal expansion coefficient have not been reported.

Simulations have explored how phosphonium ILs interact with water and CO_2. These studies have shown that the presence of chemical species can affect anion-cation interactions, which in turn may affect properties like density and self-diffusion. However, there are few studies on how properties like viscosity change due to the presence of other fluids, particularly water that is known to be introduced during IL synthesis. There may also be other impurities, such as halogens, introduced during the synthesis process that could affect material properties and lubrication performance. Impurities could be modeled explicitly both to improve the consistency of predicted and measured values, as well as explore the atomic interactions between ions and impurities. Finally, when phosphonium ILs are used as additives in oil-based lubricant formulations, they will necessarily interact with base oil molecules as well as other additives. Simulations could explore such interactions in future studies and, using the results from existing studies with water and CO_2 as a baseline, gain a fundamental understanding of these interactions.

Beyond the properties of the ILs themselves, the effectiveness of lubricants will depend on their response to confinement and interactions with solid materials. Studies of non-phosphonium ILs confined between solid wall have already shown this is a rich area of research. For example, differences in tribological behavior were reported for fatty acid ILs between steel-steel, steel-aluminum, steel-bronze, and steel-tungsten carbide [169]. Studies of ammonium and imidazolium ILs confined

between various materials have shown that friction is affected by surface polarity, roughness, and charge because these factors affected the orientation and order of the ions [152–156, 170, 171]. It was also shown that water adsorption affects the friction and film thickness of [BMIM][PF_6] confined between charged surfaces [156]. Future MD simulations could use similar methods to model phosphonium ILs with different solid materials to explore interactions between the ILs and surfaces, and the corresponding frictional behavior. Although more challenging because of the length scale limitations of MD, simulations that explore the ability of ILs to minimize wear would also be valuable.

Finally, most of the studies performed so far have used non-reactive, non-polarizable force fields. These force fields are suitable for calculating some material properties and interactions. Polarizable force fields have been found to be more accurate than non-polarizable force field, but they are only available for a small number of cation-anion pairs. Therefore, parameterization of polarizable force fields would increase the variety of ILs that can be accurately modeled. In addition, for properties or processes that involve the chemical bond dissociation formation, a reactive force field is required. If additional reactive force field parameters could be developed for ILs, this would make possible make more simulations to study important properties, such as chemical degradation that directly affects the durability of phosphonium ILs or chemical reactions with additives in a fully formulated lubricant.

5 Conclusions

This review has summarized research performed using MD simulations to explore the lubricant-relevant properties of phosphonium ILs. Many studies have focused on physico-chemical properties because these properties are important for multiple current and potential applications of ILs. The primary goal of such simulations has been to predict, validate if possible, and then explain the atomic-scale mechanisms underlying observed trends, particularly the relationship between cation-anion pair and properties. And, although the scope of this review was limited to phosphonium ILs, many of the trends discussed are relevant to other cations. While simulations that include other chemical species or solid walls are still rare, they are exciting because IL lubricant performance will certainly be affected by the interactions between ILs and their environment. The availability of reactive potentials is also a promising direction of research, since it opens the possibility of exploring properties and processes that involve chemical reactions. For both reactive and non-reactive force fields, extending parameter sets to increase the number and variety of ILs that can be modeled and simulated. Phosphonium ILs and their mixture with other species under real lubrication conditions will be critical to the continued development of this research area. As identified throughout this review, there are many opportunities for future research and there is now a strong foundation of simulation and analysis methods on which the research community can build. We hope this review has demonstrated the significant potential for simulations to play an important role in the development of phosphonium ILs as environmentally benign lubricants and additives.

6 Ionic Liquid Abbreviations

The following are abbreviations used for cations and anions within the body of the document.

P1,1,1,1	tetramethylphosphonium
P1,1,1,6	hexyltrimethylphosphonium
P2,2,2,2	tetraethylphosphonium
P2,2,2,5	triethylpentylphosphonium
P2,2,2,8	triethyloctylphosphonium
P2,2,2,12	triethyldodecylphosphonium
P2,2,2,1O1	triethyl(methoxymethyl)phosphonium
P2,2,2,2O1	triethyl(2-methoxyethyl)phosphonium
P3,3,3,3	tetrapropylphosphonium
P4,4,4,4	tetrabutylphosphonium
P4,4,4,8	tributyloctylphosphonium
P4,4,4,14	tributyltetradecylphosphonium
P6,6,6,6	tetrahexylphosphonium
P6,6,6,14	trihexyltetradecylphosphonium
P8,8,8,8	tetraoctylphosphonium
$HP(Ph)_3$	triphenylphosphonium
$HP(Oct)_3$	trioctylphosphonium
$P2(Ph)_3$	ethyltriphenylphosphonium
$P3(Ph)_3$	propyltriphenylphosphonium
$P4(Ph)_3$	butyltriphenylphosphonium
$P6(Ph)_3$	hexyltriphenylphosphonium
$P8(Ph)_3$	octyltriphenylphosphonium
β-Ala	β-alaninate
2-CNpyr	2-cyanopyrrolide
3-Triaz	1,2,3-triazolide
AcO	acetate
Ala	alaninate
Asp	aspartic acid (aspartate)
Benz	benzoate
Benzim	benzimidazolide
BF_4	tetrafluoroborate
BMB	bis(mandelato)borate
BMIM	1-butyl-3-methylimidazolium
BMLB	bis(malonato)borate
BnIm	Benzodimidazolide
BOB	bis(oxalato)borate
Br	bromide
BrBnIm	6-Bromo-benzimidazolide
BScB	bis(salicylato)borate
ButO	butanoate
CF_3pyra	2-(Trifluoromethyl)pyrazolide

Cl	chloride
DCA	dicyanamide
DecO	decanoate
DEP	diethyl phosphate
EMIM	1-Ethyl-3-methylimidazolium
FAP	tris(pentafluoroethyl)trifluorophosphate
Gln	glutaminate
Glu	glutamate
Gly	glycinate
HexO	hexanoate
Ido	1,3-indanedionate
Ile	isoleucinate
Im	Imidazolide
Leu	leucinate
Lys	lysinate
$MeSO_4$	methyl sulfate
Met	methioninate
MMIM	1,3-dimethylimidazolium
OctO	octanoate
OTf	triflate
PF_6	hexafluorophosphate
Phe	phenylalaninate
PhO	phenolate
Pro	prolinate
Sali	salicylate
Ser	serinate
Tau	taurinate
Tf_2N	bis(trifluoromethanesulfonyl)imide
TFA	trifluoroacetate
TFO	triflate
TFSI	bis(trifluoromethyl)sulfonylimide
Thr	threonate
TMPP	bis(2,4,4-trimethylpentyl)phosphinate
Val	valinate

7 Acknowledgments

The authors acknowledge the support of the National Science Foundation (Grant No. CMMI-2010205 and 2010584).

References

[1] Joshi, M.D., Anderson, J.L.: Recent advances of ionic liquids in separation science and mass spectrometry. RSC Adv. **2**(13), 5470–5484 (2012)

[2] Singh, S.K., Savoy, A.W.: Ionic liquids synthesis and applications: An overview. J. Mol. Liq. **297**, 112038 (2020)

[3] Rahman, M.H., Khajeh, A., Panwar, P., Patel, M., Martini, A., Menezes, P.L.: Recent progress on phosphonium-based room temperature ionic liquids: Synthesis, properties, tribological performances and applications. Tribol. Int. **167**, 107331 (2022)

[4] Liu, X., Zhou, F., Liang, Y., Liu, W.: Tribological performance of phosphonium based ionic liquids for an aluminum-on-steel system and opinions on lubrication mechanism. Wear **261**(10), 1174–1179 (2006)

[5] Weng, L., Liu, X., Liang, Y., Xue, Q.: Effect of tetraalkylphosphonium based ionic liquids as lubricants on the tribological performance of a steel-on-steel system. Tribol. Lett. **26**(1), 11–17 (2007)

[6] Minami, I., Kita, M., Kubo, T., Nanao, H., Mori, S.: The tribological properties of ionic liquids composed of trifluorotris (pentafluoroethyl) phosphate as a hydrophobic anion. Tribol. Lett. **30**(3), 215–223 (2008)

[7] Minami, I., Inada, T., Sasaki, R., Nanao, H.: Tribo-chemistry of phosphonium-derived ionic liquids. Tribol. Lett. **40**(2), 225–235 (2010)

[8] Scarbath-Evers, L.K., Hunt, P.A., Kirchner, B., MacFarlane, D.R., Zahn, S.: Molecular features contributing to the lower viscosity of phosphonium ionic liquids compared to their ammonium analogues. Phys. Chem. Chem. Phys. **17**(31), 20205–20216 (2015)

[9] Naik, P.K., Paul, S., Banerjee, T.: Physiochemical properties and molecular dynamics simulations of phosphonium and ammonium based deep eutectic solvents. J. Solution Chem. **48**(7), 1046–1065 (2019)

[10] Otero, I., Loépez, E.R., Reichelt, M., Villanueva, M., Salgado, J., Fernaéndez, J.: Ionic liquids based on phosphonium cations as neat lubricants or lubricant additives for a steel/steel contact. ACS Appl. Mater. Interfaces **6**(15), 13115–13128 (2014)

[11] Fraser, K.J., MacFarlane, D.R.: Phosphonium-based ionic liquids: an overview. Aust. J. Chem. **62**(4), 309–321 (2009)

[12] Maton, C., De Vos, N., Stevens, C.V.: Ionic liquid thermal stabilities: decomposition mechanisms and analysis tools. Chem. Soc. Rev. **42**(13), 5963–5977 (2013)

[13] Khazalpour, S., Yarie, M., Kianpour, E., Amani, A., Asadabadi, S., Seyf, J.Y.,

Rezaeivala, M., Azizian, S., Zolfigol, M.A.: Applications of phosphonium-based ionic liquids in chemical processes. J. Iran. Chem. Soc. **17**(8), 1775–1917 (2020)

[14] Yu, B., Bansal, D.G., Qu, J., Sun, X., Luo, H., Dai, S., Blau, P.J., Bunting, B.G., Mordukhovich, G., Smolenski, D.J.: Oil-miscible and non-corrosive phosphonium-based ionic liquids as candidate lubricant additives. Wear **289**, 58–64 (2012)

[15] Cai, M., Yu, Q., Liu, W., Zhou, F.: Ionic liquid lubricants: When chemistry meets tribology. Chem. Soc. Rev. (2020)

[16] Henriques, R.R., Soares, B.G.: Sepiolite modified with phosphonium ionic liquids as anticorrosive pigment for epoxy coatings. Appl. Clay Sci. **200**, 105890 (2021)

[17] Shah, F.U., Glavatskih, S., MacFarlane, D.R., Somers, A., Forsyth, M., Antzutkin, O.N.: Novel halogen-free chelated orthoborate–phosphonium ionic liquids: synthesis and tribophysical properties. Phys. Chem. Chem. Phys. **13**(28), 12865–12873 (2011)

[18] Totolin, V., Minami, I., Gabler, C., Dörr, N.: Halogen-free borate ionic liquids as novel lubricants for tribological applications. Tribol. Int. **67**, 191–198 (2013)

[19] Zhu, L., Dong, J., Ma, Y., Jia, Y., Peng, C., Li, W., Zhang, M., Gong, K., Wang, X.: Synthesis and investigation of halogen-free phosphonium-based ionic liquids for lubrication applications. Tribol. Trans. **62**(6), 943–954 (2019)

[20] Sydow, M., Owsianiak, M., Framski, G., Woźniak-Karczewska, M., Piotrowska-Cyplik, A., Ławniczak, Ł., Szulc, A., Zgoła-Grześkowiak, A., Heipieper, H.J., Chrzanowski, Ł.: Biodiversity of soil bacteria exposed to sublethal concentrations of phosphonium-based ionic liquids: Effects of toxicity and biodegradation. Ecotoxicol. Environ. Saf. **147**, 157–164 (2018)

[21] Oulego, P., Blanco, D., Ramos, D., Viesca, J., Díaz, M., Battez, A.H.: Environmental properties of phosphonium, imidazolium and ammonium cation-based ionic liquids as potential lubricant additives. J. Mol. Liq. **272**, 937–947 (2018)

[22] Rohlmann, P., Munavirov, B., Furó, I., Antzutkin, O., Rutland, M.W., Glavatskih, S.: Non-halogenated ionic liquid dramatically enhances tribological performance of biodegradable oils. Front. Chem. **7**, 98 (2019)

[23] Zhou, Y., Qu, J.: Ionic liquids as lubricant additives: a review. ACS Appl. Mater. Interfaces **9**(4), 3209–3222 (2017)

[24] Kasar, A.K., Reeves, C.J., Menezes, P.L.: The effect of particulate additive

mixtures on the tribological performance of phosphonium-based ionic liquid lubricants. Tribol. Int. **165**, 107300 (2022)

[25] Sivapragasam, M., Jaganathan, J.R., Levêque, J.-M., Moniruzzaman, M., Mutalib, M.A.: Microbial biocompatibility of phosphonium-and ammonium-based ionic liquids. J. Mol. Liq. **273**, 107–115 (2019)

[26] Reeves, C.J., Siddaiah, A., Menezes, P.L.: Tribological study of imidazolium and phosphonium ionic liquid-based lubricants as additives in carboxylic acid-based natural oil: advancements in environmentally friendly lubricants. J. Cleaner Prod. **176**, 241–250 (2018)

[27] Yang, J., Zhou, Z., Liang, Y., Tang, J., Gao, Y., Niu, J., Dong, H., Tang, R., Tang, G., Cao, Y.: Sustainable preparation of microcapsules with desirable stability and bioactivity using phosphonium ionic liquid as a functional additive. ACS Sustainable Chem. Eng. **8**(35), 13440–13448 (2020)

[28] Nazir, S., Khawar Rauf, M., Ebihara, M., Hameed, S.: [4-(methoxycarbonyl) benzyl] triphenylphosphonium bromide hemihydrate. Acta Crystallogr., Sect. E: Struct. Rep. Online **64**(2), 423–423 (2008)

[29] Dove, M.T.: An introduction to atomistic simulation methods. Seminarios de la SEM **4**, 7–37 (2008)

[30] Balluffi, R.W., Allen, S.M., Carter, W.C.: Kinetics of Materials. John Wiley & Sons, ??? (2005)

[31] Allen, M.P., Tildesley, D.J.: Computer Simulation of Liquids. Oxford university press, Oxford (2017)

[32] Yan, T., Burnham, C.J., Del Pópolo, M.G., Voth, G.A.: Molecular dynamics simulation of ionic liquids: The effect of electronic polarizability. J. Phys. Chem. B **108**(32), 11877–11881 (2004)

[33] Borodin, O.: Polarizable force field development and molecular dynamics simulations of ionic liquids. J. Phys. Chem. B **113**(33), 11463–11478 (2009)

[34] Starovoytov, O.N., Torabifard, H., Cisneros, G.A.: Development of amoeba force field for 1, 3-dimethylimidazolium based ionic liquids. J. Phys. Chem. B **118**(25), 7156–7166 (2014)

[35] Wang, Y.-L., Shah, F.U., Glavatskih, S., Antzutkin, O.N., Laaksonen, A.: Atomistic insight into orthoborate-based ionic liquids: force field development and evaluation. J. Phys. Chem. B **118**(29), 8711–8723 (2014)

[36] Bedrov, D., Piquemal, J.-P., Borodin, O., MacKerell Jr, A.D., Roux, B., Shroder, C.: Molecular dynamics simulations of ionic liquids and electrolytes

using polarizable force fields. Chem. Rev. **119**(13), 7940–7995 (2019)

[37] Goloviznina, K., Canongia Lopes, J.N., Costa Gomes, M., Pádua, A.A.: Transferable, polarizable force field for ionic liquids. J. Chem. Theory Comput. **15**(11), 5858–5871 (2019)

[38] Vázquez-Montelongo, E.A., Vázquez-Cervantes, J.E., Cisneros, G.A.: Current status of amoeba–il: A multipolar/polarizable force field for ionic liquids. Int. J. Mol. Sci. **21**(3), 697 (2020)

[39] Canongia Lopes, J.N., Deschamps, J., Pádua, A.A.: Modeling ionic liquids using a systematic all-atom force field. J. Phys. Chem. B **108**(6), 2038–2047 (2004)

[40] Canongia Lopes, J.N., Pádua, A.A.: Molecular force field for ionic liquids composed of triflate or bistriflylimide anions. J. Phys. Chem. B **108**(43), 16893–16898 (2004)

[41] Canongia Lopes, J.N., Pádua, A.A.: Molecular force field for ionic liquids iii: Imidazolium, pyridinium, and phosphonium cations; chloride, bromide, and dicyanamide anions. J. Phys. Chem. B **110**(39), 19586–19592 (2006)

[42] Canongia Lopes, J.N., Pádua, A.A., Shimizu, K.: Molecular force field for ionic liquids iv: Trialkylimidazolium and alkoxycarbonyl-imidazolium cations; alkylsulfonate and alkylsulfate anions. J. Phys. Chem. B **112**(16), 5039–5046 (2008)

[43] Shimizu, K., Almantariotis, D., Gomes, M.F.C., Padua, A.A., Canongia Lopes, J.N.: Molecular force field for ionic liquids v: Hydroxyethylimidazolium, dimethoxy-2-methylimidazolium, and fluoroalkylimidazolium cations and bis (fluorosulfonyl) amide, perfluoroalkanesulfonylamide, and fluoroalkylfluorophosphate anions. J. Phys. Chem. B **114**(10), 3592–3600 (2010)

[44] Lopes, J.N.C., Pádua, A.A.: Cl&p: A generic and systematic force field for ionic liquids modeling. Theor. Chem. Acc. **131**(3), 1–11 (2012)

[45] Xia, M., Chai, Z., Wang, D.: Polarizable and non-polarizable force field representations of ferric cation and validations. J. Phys. Chem. B **121**(23), 5718–5729 (2017)

[46] Cornell, W.D., Cieplak, P., Bayly, C.I., Gould, I.R., Merz, K.M., Ferguson, D.M., Spellmeyer, D.C., Fox, T., Caldwell, J.W., Kollman, P.A.: A second generation force field for the simulation of proteins, nucleic acids, and organic molecules. J. Am. Chem. Soc. **117**(19), 5179–5197 (1995)

[47] Jorgensen, W.L., Maxwell, D.S., Tirado-Rives, J.: Development and testing of the opls all-atom force field on conformational energetics and properties of

organic liquids. J. Am. Chem. Soc. **118**(45), 11225–11236 (1996)

[48] Liu, Z., Huang, S., Wang, W.: A refined force field for molecular simulation of imidazolium-based ionic liquids. J. Phys. Chem. B **108**(34), 12978–12989 (2004)

[49] Wu, X., Liu, Z., Huang, S., Wang, W.: Molecular dynamics simulation of room-temperature ionic liquid mixture of [bmim][bf4] and acetonitrile by a refined force field. Phys. Chem. Chem. Phys. **7**(14), 2771–2779 (2005)

[50] Zhou, G., Liu, X., Zhang, S., Yu, G., He, H.: A force field for molecular simulation of tetrabutylphosphonium amino acid ionic liquids. J. Phys. Chem. B **111**(25), 7078–7084 (2007)

[51] Wu, H., Shah, J.K., Tenney, C.M., Rosch, T.W., Maginn, E.J.: Structure and dynamics of neat and co2-reacted ionic liquid tetrabutylphosphonium 2-cyanopyrrolide. Ind. Eng. Chem. Res. **50**(15), 8983–8993 (2011)

[52] Parker, Q., Bell, R.G., de Leeuw, N.H.: Structural and dynamical properties of ionic liquids: a molecular dynamics study employing dl_poly 4. Mol. Simul., 1–9 (2019)

[53] Sheridan, Q.R., Schneider, W.F., Maginn, E.J.: Role of molecular modeling in the development of co2–reactive ionic liquids. Chem. Rev. **118**(10), 5242–5260 (2018)

[54] Sambasivarao, S.V., Acevedo, O.: Development of opls-aa force field parameters for 68 unique ionic liquids. J. Chem. Theory Comput. **5**(4), 1038–1050 (2009)

[55] Doherty, B., Zhong, X., Gathiaka, S., Li, B., Acevedo, O.: Revisiting opls force field parameters for ionic liquid simulations. J. Chem. Theory Comput. **13**(12), 6131–6145 (2017)

[56] Dommert, F., Holm, C.: Refining classical force fields for ionic liquids: theory and application to [mmim][cl]. Phys. Chem. Chem. Phys. **15**(6), 2037–2049 (2013)

[57] Voroshylova, I.V., Chaban, V.V.: Atomistic force field for pyridinium-based ionic liquids: reliable transport properties. J. Phys. Chem. B **118**(36), 10716–10724 (2014)

[58] Chaban, V.V., Voroshylova, I.V.: Systematic refinement of canongia lopes–pádua force field for pyrrolidinium-based ionic liquids. J. Phys. Chem. B **119**(20), 6242–6249 (2015)

[59] Köddermann, T., Paschek, D., Ludwig, R.: Molecular dynamic simulations

of ionic liquids: A reliable description of structure, thermodynamics and dynamics. ChemPhysChem **8**(17), 2464–2470 (2007)

[60] Vergadou, N., Androulaki, E., Hill, J.-R., Economou, I.G.: Molecular simulations of imidazolium-based tricyanomethanide ionic liquids using an optimized classical force field. Phys. Chem. Chem. Phys. **18**(9), 6850–6860 (2016)

[61] Liu, X., Zhou, G., Zhang, S., Yu, G.: Molecular simulations of phosphonium-based ionic liquid. Mol. Simul. **36**(1), 79–86 (2010)

[62] Liu, X., Zhao, Y., Zhang, X., Zhou, G., Zhang, S.: Microstructures and interaction analyses of phosphonium-based ionic liquids: a simulation study. J. Phys. Chem. B **116**(16), 4934–4942 (2012)

[63] Wang, Y.-L., Sarman, S., Kloo, L., Antzutkin, O.N., Glavatskih, S., Laaksonen, A.: Solvation structures of water in trihexyltetradecylphosphonium-orthoborate ionic liquids. J. Chem. Phys. **145**(6), 064507 (2016)

[64] Sarman, S., Wang, Y.-L., Rohlmann, P., Glavatskih, S., Laaksonen, A.: Rheology of phosphonium ionic liquids: a molecular dynamics and experimental study. Phys. Chem. Chem. Phys. **20**(15), 10193–10203 (2018)

[65] Pereira, G.F.L., Pereira, R.G., Salanne, M., Siqueira, L.J.A.: Molecular dynamics simulations of ether-modified phosphonium ionic liquid confined in between planar and porous graphene electrode models. J. Phys. Chem. C **123**(17), 10816–10825 (2019)

[66] Van Duin, A.C., Dasgupta, S., Lorant, F., Goddard, W.A.: Reaxff: a reactive force field for hydrocarbons. J. Phys. Chem. A **105**(41), 9396–9409 (2001)

[67] Zhang, B., van Duin, A.C., Johnson, J.K.: Development of a reaxff reactive force field for tetrabutylphosphonium glycinate/co2 mixtures. J. Phys. Chem. B **118**(41), 12008–12016 (2014)

[68] Tsuzuki, S., Tokuda, H., Hayamizu, K., Watanabe, M.: Magnitude and directionality of interaction in ion pairs of ionic liquids: Relationship with ionic conductivity. J. Phys. Chem. B **109**(34), 16474–16481 (2005)

[69] Maschio, L., Civalleri, B., Ugliengo, P., Gavezzotti, A.: Intermolecular interaction energies in molecular crystals: comparison and agreement of localized møller–plesset 2, dispersion-corrected density functional, and classical empirical two-body calculations. J. Phys. Chem. A **115**(41), 11179–11186 (2011)

[70] Gontrani, L., Russina, O., Lo Celso, F., Caminiti, R., Annat, G., Triolo, A.: Liquid structure of trihexyltetradecylphosphonium chloride at ambient temperature: An x-ray scattering and simulation study. J. Phys. Chem. B **113**(27),

9235–9240 (2009)

[71] Martins, V.L., Sanchez-Ramirez, N., Ribeiro, M.C., Torresi, R.M.: Two phosphonium ionic liquids with high li+ transport number. Phys. Chem. Chem. Phys. **17**(35), 23041–23051 (2015)

[72] Shaikh, A.R., Ashraf, M., AlMayef, T., Chawla, M., Poater, A., Cavallo, L.: Amino acid ionic liquids as potential candidates for co2 capture: combined density functional theory and molecular dynamics simulations. Chem. Phys. Lett. **745**, 137239 (2020)

[73] Zhao, Y., Tian, L., Pei, Y., Wang, H., Wang, J.: Effect of anionic structure on the lcst phase behavior of phosphonium ionic liquids in water. Ind. Eng. Chem. Res. **57**(38), 12935–12941 (2018)

[74] Zhang, X., Huo, F., Liu, X., Dong, K., He, H., Yao, X., Zhang, S.: Influence of microstructure and interaction on viscosity of ionic liquids. Ind. Eng. Chem. Res. **54**(13), 3505–3514 (2015)

[75] Laaksonen, A., Kusalik, P., Svishchev, I.: Three-dimensional structure in water- methanol mixtures. J. Phys. Chem. A **101**(33), 5910–5918 (1997)

[76] Kulińska, K., Kuliński, T., Lyubartsev, A., Laaksonen, A., Adamiak, R.W.: Spatial distribution functions as a tool in the analysis of ribonucleic acids hydration—molecular dynamics studies. Comput. Chem. **24**(3-4), 451–457 (2000)

[77] Kusalik, P.G., Svishchev, I.M.: The spatial structure in liquid water. Science **265**(5176), 1219–1221 (1994)

[78] Gillespie, R.J., Popelier, P.L.A.: Chemical Bonding and Molecular Geometry. Oxford University Press, ??? (2001)

[79] Dong, K., Zhang, S.: Hydrogen bonds: a structural insight into ionic liquids. Chem. - Eur. J. **18**(10), 2748–2761 (2012)

[80] Luo, J., Conrad, O., Vankelecom, I.F.: Physicochemical properties of phosphonium-based and ammonium-based protic ionic liquids. J. Mater. Chem. **22**(38), 20574–20579 (2012)

[81] Guardia, E., Martí, J., García-Tarrés, L., Laria, D.: A molecular dynamics simulation study of hydrogen bonding in aqueous ionic solutions. J. Mol. Liq. **117**(1-3), 63–67 (2005)

[82] Fitch, E.C.: Proactive Maintenance for Mechanical Systems vol. 5. Elsevier, Stillwater (2013)

[83] Quercia, G., Belisario, R., Rengifo, R.: Reduction of erosion rate by particle size distribution (psd) modification of hematite as weighting agent for oil based drilling fluids. Wear **266**(11-12), 1229–1236 (2009)

[84] Gao, X., Fang, J., Wang, H.: Sampling the isothermal-isobaric ensemble by langevin dynamics. J. Chem. Phys. **144**(12), 124113 (2016)

[85] Wu, H., Maginn, E.J.: Water solubility and dynamics of co2 capture ionic liquids having aprotic heterocyclic anions. Fluid Phase Equilib. **368**, 72–79 (2014)

[86] Wang, Y.-L., Shimpi, M.R., Sarman, S., Antzutkin, O.N., Glavatskih, S., Kloo, L., Laaksonen, A.: Atomistic insight into tetraalkylphosphonium bis (oxalato) borate ionic liquid/water mixtures. 2. volumetric and dynamic properties. J. Phys. Chem. B **120**(30), 7446–7455 (2016)

[87] Venkatesan, S.S., Huda, M.M., Rai, N.: Molecular insights into ionic liquid/aqueous interface of phosphonium based phase-separable ionic liquids. AIP Adv. **9**(4), 045115 (2019)

[88] Sharma, S., Gupta, A., Dhabal, D., Kashyap, H.K.: Pressure-dependent morphology of trihexyl (tetradecyl) phosphonium ionic liquids: A molecular dynamics study. J. Chem. Phys. **145**(13), 134506 (2016)

[89] Mondal, A., Sunda, A.P.: Molecular dynamics simulations of ammonium/phosphonium-based protic ionic liquids: influence of alkyl to aryl group. Phys. Chem. Chem. Phys. **20**(28), 19268–19275 (2018)

[90] Shimpi, M.R., Rohlmann, P., Shah, F.U., Glavatskih, S., Antzutkin, O.N.: Transition anionic complex in trihexyl (tetradecyl) phosphonium-bis (oxalato) borate ionic liquid–revisited. Phys. Chem. Chem. Phys. **23**(10), 6190–6203 (2021)

[91] Kasahara, S., Kamio, E., Matsuyama, H.: Improvements in the co2 permeation selectivities of amino acid ionic liquid-based facilitated transport membranes by controlling their gas absorption properties. J. Membr. Sci. **454**, 155–162 (2014)

[92] Blahušiak, M., Schlosser, Š.: Physical properties of phosphonium ionic liquid and its mixtures with dodecane and water. J. Chem. Thermodyn. **72**, 54–64 (2014)

[93] Marták, J., Schlosser, S.: Density, viscosity, and structure of equilibrium solvent phases in butyric acid extraction by phosphonium ionic liquid. J. Chem. Eng. Data **62**(10), 3025–3035 (2017)

[94] Oster, K., Goodrich, P., Jacquemin, J., Hardacre, C., Ribeiro, A., Elsinawi, A.:

A new insight into pure and water-saturated quaternary phosphonium-based carboxylate ionic liquids: Density, heat capacity, ionic conductivity, thermogravimetric analysis, thermal conductivity and viscosity. J. Chem. Thermodyn. **121**, 97–111 (2018)

[95] Seo, S., DeSilva, M.A., Xia, H., Brennecke, J.F.: Effect of cation on physical properties and co2 solubility for phosphonium-based ionic liquids with 2-cyanopyrrolide anions. J. Phys. Chem. B **119**(35), 11807–11814 (2015)

[96] Kolbeck, C., Lehmann, J., Lovelock, K., Cremer, T., Paape, N., Wasserscheid, P., Froba, A., Maier, F., Steinruck, H.-P.: Density and surface tension of ionic liquids. J. Phys. Chem. B **114**(51), 17025–17036 (2010)

[97] Tariq, M., Forte, P., Gomes, M.C., Lopes, J.C., Rebelo, L.: Densities and refractive indices of imidazolium-and phosphonium-based ionic liquids: Effect of temperature, alkyl chain length, and anion. J. Chem. Thermodyn. **41**(6), 790–798 (2009)

[98] Seki, S., Kobayashi, T., Kobayashi, Y., Takei, K., Miyashiro, H., Hayamizu, K., Tsuzuki, S., Mitsugi, T., Umebayashi, Y.: Effects of cation and anion on physical properties of room-temperature ionic liquids. J. Mol. Liq. **152**(1-3), 9–13 (2010)

[99] Montalbán, M., Bolívar, C., Diaz Banos, F.G., Víllora, G.: Effect of temperature, anion, and alkyl chain length on the density and refractive index of 1-alkyl-3-methylimidazolium-based ionic liquids. J. Chem. Eng. Data **60**(7), 1986–1996 (2015)

[100] Ebrahimi, M., Moosavi, F.: The effects of temperature, alkyl chain length, and anion type on thermophysical properties of the imidazolium based amino acid ionic liquids. J. Mol. Liq. **250**, 121–130 (2018)

[101] Hess, B.: Determining the shear viscosity of model liquids from molecular dynamics simulations. J. Chem. Phys. **116**(1), 209–217 (2002)

[102] Ramasamy, U.S., Len, M., Martini, A.: Correlating molecular structure to the behavior of linear styrene–butadiene viscosity modifiers. Tribol. Lett. **65**(4), 1–8 (2017)

[103] Len, M., Ramasamy, U.S., Lichter, S., Martini, A.: Thickening mechanisms of polyisobutylene in polyalphaolefin. Tribol. Lett. **66**(1), 1–9 (2018)

[104] Panwar, P., Michael, P., Devlin, M., Martini, A.: Critical shear rate of polymer-enhanced hydraulic fluids. Lubricants **8**(12), 102 (2020)

[105] Mathas, D., Holweger, W., Wolf, M., Bohnert, C., Bakolas, V., Procelewska, J., Wang, L., Bair, S., Skylaris, C.-K.: Evaluation of methods for viscosity

simulations of lubricants at different temperatures and pressures: a case study on pao-2. Tribol. Trans. (just-accepted), 1–26 (2021)

[106] Noda, A., Hayamizu, K., Watanabe, M.: Pulsed-gradient spin- echo 1h and 19f nmr ionic diffusion coefficient, viscosity, and ionic conductivity of non-chloroaluminate room-temperature ionic liquids. J. Phys. Chem. B **105**(20), 4603–4610 (2001)

[107] Ghatee, M.H., Bahrami, M.: Emergence of innovative properties by replacement of nitrogen atom with phosphorus atom in quaternary ammonium ionic liquids: Insights from ab initio calculations and md simulations. Chem. Phys. **490**, 92–105 (2017)

[108] J Evans, D., P Morriss, G.: Statistical Mechanics of Nonequilbrium Liquids. ANU Press, Canberra (2007)

[109] Li, A., Tian, Z., Yan, T., Jiang, D.-e., Dai, S.: Anion-functionalized task-specific ionic liquids: molecular origin of change in viscosity upon co2 capture. J. Phys. Chem. B **118**(51), 14880–14887 (2014)

[110] Firaha, D.S., Gibalova, A.V., Holloczki, O.: Basic phosphonium ionic liquids as wittig reagents. ACS omega **2**(6), 2901–2911 (2017)

[111] Barnhill, W.C., Qu, J., Luo, H., Meyer III, H.M., Ma, C., Chi, M., Papke, B.L.: Phosphonium-organophosphate ionic liquids as lubricant additives: effects of cation structure on physicochemical and tribological characteristics. ACS Appl. Mater. Interfaces **6**(24), 22585–22593 (2014)

[112] Rauber, D., Zhang, P., Huch, V., Kraus, T., Hempelmann, R.: Lamellar structures in fluorinated phosphonium ionic liquids: the roles of fluorination and chain length. Phys. Chem. Chem. Phys. **19**(40), 27251–27258 (2017)

[113] Yamaguchi, T.: Shear thinning and nonlinear structural deformation of ionic liquids with long alkyl chains studied by molecular dynamics simulation. J. Phys. Chem. B **123**(29), 6260–6265 (2019)

[114] Ma, Y., Liu, Y., Su, H., Wang, L., Zhang, J.: Relationship between hydrogen bond and viscosity for a series of pyridinium ionic liquids: Molecular dynamics and quantum chemistry. J. Mol. Liq. **255**, 176–184 (2018)

[115] Santos, E., Albo, J., Daniel, C., Portugal, C., Crespo, J., Irabien, A.: Permeability modulation of supported magnetic ionic liquid membranes (smilms) by an external magnetic field. Journal of membrane science **430**, 56–61 (2013)

[116] Lourenço, T.C., Zhang, Y., Costa, L.T., Maginn, E.J.: A molecular dynamics study of lithium-containing aprotic heterocyclic ionic liquid electrolytes. J. Chem. Phys. **148**(19), 193834 (2018)

[117] Sheridan, Q.R., Schneider, W.F., Maginn, E.J.: Anion dependent dynamics and water solubility explained by hydrogen bonding interactions in mixtures of water and aprotic heterocyclic anion ionic liquids. J. Phys. Chem. B **120**(49), 12679–12686 (2016)

[118] Huang, W., Kong, L., Wang, X.: Electrical sliding friction lubricated with ionic liquids. Tribol. Lett. **65**(1), 1–6 (2017)

[119] Gonda, A., Capan, R., Bechev, D., Sauer, B.: The influence of lubricant conductivity on bearing currents in the case of rolling bearing greases. Lubricants **7**(12), 108 (2019)

[120] Chen, Y., Jha, S., Raut, A., Zhang, W., Liang, H.: Performance characteristics of lubricants in electric and hybrid vehicles: a review of current and future needs. Front. Mech. Eng. **6**, 82 (2020)

[121] Harada, M., Yamanaka, A., Tanigaki, M., Tada, Y.: Mass and size effects on the transport properties of molten salts. J. Chem. Phys. **76**(3), 1550–1556 (1982)

[122] Basouli, H., Mozaffari, F., Eslami, H.: Atomistic insights into structure, ion-pairing and ionic conductivity of 1-ethyl-3-methylimidazolium methylsulfate [emim][meso4] ionic liquid from molecular dynamics simulation. J. Mol. Liq. **331**, 115803 (2021)

[123] Hansen, J.-P., McDonald, I.R.: Theory of Simple Liquids: with Applications to Soft Matter. Academic press, ??? (2013)

[124] Mao, Y., Zhang, Y.: Thermal conductivity, shear viscosity and specific heat of rigid water models. Chem. Phys. Lett. **542**, 37–41 (2012)

[125] Gardas, R.L., Ge, R., Goodrich, P., Hardacre, C., Hussain, A., Rooney, D.W.: Thermophysical properties of amino acid-based ionic liquids. J. Chem. Eng. Data **55**(4), 1505–1515 (2010)

[126] Ferreira, A.F., Simões, P.N., Ferreira, A.G.: Quaternary phosphonium-based ionic liquids: Thermal stability and heat capacity of the liquid phase. J. Chem. Thermodyn. **45**(1), 16–27 (2012)

[127] Oster, K., Jacquemin, J., Hardacre, C., Ribeiro, A., Elsinawi, A.: Further development of the predictive models for physical properties of pure ionic liquids: Thermal conductivity and heat capacity. J. Chem. Thermodyn. **118**, 1–15 (2018)

[128] Zhai, L., Zhong, Q., He, C., Wang, J.: Hydroxyl ammonium ionic liquids synthesized by water-bath microwave: Synthesis and desulfurization. J. Hazard. Mater. **177**(1-3), 807–813 (2010)

[129] Adamová, G., Gardas, R.L., Rebelo, L.P.N., Robertson, A.J., Seddon, K.R.: Alkyltrioctylphosphonium chloride ionic liquids: synthesis and physicochemical properties. Dalton Trans. **40**(47), 12750–12764 (2011)

[130] Montanino, M., Alessandrini, F., Passerini, S., Appetecchi, G.B.: Water-based synthesis of hydrophobic ionic liquids for high-energy electrochemical devices. Electrochim. Acta **96**, 124–133 (2013)

[131] Verma, C., Ebenso, E.E., Quraishi, M.: Transition metal nanoparticles in ionic liquids: Synthesis and stabilization. J. Mol. Liq. **276**, 826–849 (2019)

[132] Dong, R., Yu, Q., Bai, Y., Wu, Y., Ma, Z., Zhang, J., Zhang, C., Yu, B., Zhou, F., Liu, W., *et al.*: Towards superior lubricity and anticorrosion performances of proton-type ionic liquids additives for water-based lubricating fluids. Chem. Eng. J. **383**, 123201 (2020)

[133] Wang, Y.-L., Sarman, S., Glavatskih, S., Antzutkin, O.N., Rutland, M.W., Laaksonen, A.: Atomistic insight into tetraalkylphosphonium-bis (oxalato) borate ionic liquid/water mixtures. i. local microscopic structure. J. Phys. Chem. B **119**(16), 5251–5264 (2015)

[134] Kroon, M.C., Buijs, W., Peters, C.J., Witkamp, G.-J.: Quantum chemical aided prediction of the thermal decomposition mechanisms and temperatures of ionic liquids. Thermochim. Acta **465**(1-2), 40–47 (2007)

[135] Golets, M., Shimpi, M., Wang, Y.-L., Antzutkin, O., Glavatskih, S., Laaksonen, A.: Understanding the thermal decomposition mechanism of a halogen-free chelated orthoborate-based ionic liquid: a combined computational and experimental study. Phys. Chem. Chem. Phys. **18**(32), 22458–22466 (2016)

[136] Sun, Z., Pan, J., Guo, J., Yan, F.: The alkaline stability of anion exchange membrane for fuel cell applications: the effects of alkaline media. Adv. Sci. **5**(8), 1800065 (2018)

[137] Thasneema, K., Thayyil, M.S., Rosalin, T., Elyas, K., Dipin, T., Sahu, P.K., Kumar, N.K., Saheer, V., Messali, M., Hadda, T.B.: Thermal and spectroscopic investigations on three phosphonium based ionic liquids for industrial and biological applications. J. Mol. Liq. **307**, 112960 (2020)

[138] Senftle, T.P., Hong, S., Islam, M.M., Kylasa, S.B., Zheng, Y., Shin, Y.K., Junkermeier, C., Engel-Herbert, R., Janik, M.J., Aktulga, H.M., Verstraelen, T., Grama, A., van Duin, A.C.T.: The reaxff reactive force-field: development, applications and future directions. npj Comput. Mater. **2**, 15011 (2016)

[139] Martini, A., Eder, S.J., Dörr, N.: Tribochemistry: A review of reactive molecular dynamics simulations. Lubricants **8**(4), 44 (2020)

[140] Han, S., Li, X., Guo, L., Sun, H., Zheng, M., Ge, W.: Refining fuel composition of rp-3 chemical surrogate models by reactive molecular dynamics and machine learning. Energy & Fuels **34**(9), 11381–11394 (2020)

[141] Gao, M., Li, X., Guo, L.: Pyrolysis simulations of fugu coal by large-scale reaxff molecular dynamics. Fuel Process. Technol. **178**, 197–205 (2018)

[142] Xin, L., Liu, C., Liu, Y., Huo, E., Li, Q., Wang, X., Cheng, Q.: Thermal decomposition mechanism of some hydrocarbons by reaxff-based molecular dynamics and density functional theory study. Fuel **275**, 117885 (2020)

[143] Chenoweth, K., Cheung, S., Van Duin, A.C., Goddard, W.A., Kober, E.M.: Simulations on the thermal decomposition of a poly (dimethylsiloxane) polymer using the reaxff reactive force field. J. Am. Chem. Soc. **127**(19), 7192–7202 (2005)

[144] Liu, Y., Hu, J., Hou, H., Wang, B.: Development and application of a reaxff reactive force field for molecular dynamics of perfluorinatedketones thermal decomposition. Chem. Phys. **538**, 110888 (2020)

[145] Huo, E., Liu, C., Xu, X., Dang, C.: A reaxff-based molecular dynamics study of the pyrolysis mechanism of hfo-1336mzz(z). International Journal of Refrigeration **83**, 118–130 (2017). https://doi.org/10.1016/j.ijrefrig.2017.07.009

[146] Cao, Y., Liu, C., Zhang, H., Xu, X., Li, Q.: Thermal decomposition of hfo-1234yf through reaxff molecular dynamics simulation. Appl. Therm. Eng. **126**, 330–338 (2017)

[147] Lyu, R., Huang, Z., Deng, H., Wei, Y., Mou, C., Wang, L.: Anatomies for the thermal decomposition behavior and product rule of 5,5-dinitro-2h,2h-3,3-bi-1,2,4-triazole. RSC Adv. **11**(63), 40182–40192 (2021)

[148] Lan, G., Li, J., Zhang, G., Ruan, J., Lu, Z., Jin, S., Cao, D., Wang, J.: Thermal decomposition mechanism study of 3-nitro-1, 2, 4-triazol-5-one (nto): Combined tg-ftir-ms techniques and reaxff reactive molecular dynamics simulations. Fuel **295**, 120655 (2021)

[149] Khajeh, A., Bhuiyan, F.H., Mogonye, J.-E., Pesce-Rodriguez, R.A., Berkebile, S., Martini, A.: Thermal decomposition of tricresyl phosphate on ferrous surfaces. J. Phys. Chem. C **125**(9), 5076–5087 (2021)

[150] Ewen, J.P., Latorre, C.A., Gattinoni, C., Khajeh, A., Moore, J.D., Remias, J.E., Martini, A., Dini, D.: Substituent effects on the thermal decomposition of phosphate esters on ferrous surfaces. J. Phys. Chem. C **124**(18), 9852–9865 (2020)

[151] Khajeh, A., Rahman, M.H., Liu, T., Panwar, P., Patel, M., Menezes, P.L., Martini, A.: Thermal decomposition of phosphonium salicylate and phosphonium benzoate ionic liquids. J. Mol. Liq. (2021)

[152] Mendonca, A.C., Padua, A.A., Malfreyt, P.: Nonequilibrium molecular simulations of new ionic lubricants at metallic surfaces: prediction of the friction. J. Chem. Theory Comput. **9**(3), 1600–1610 (2013)

[153] Pivnic, K., Bresme, F., Kornyshev, A.A., Urbakh, M.: Electrotunable friction in diluted room temperature ionic liquids: Implications for nanotribology. ACS Appl. Nano Mater. **3**(11), 10708–10719 (2020)

[154] Voeltzel, N., Fillot, N., Vergne, P., Joly, L.: Orders of magnitude changes in the friction of an ionic liquid on carbonaceous surfaces. J. Phys. Chem. C **122**(4), 2145–2154 (2018)

[155] Voeltzel, N., Giuliani, A., Fillot, N., Vergne, P., Joly, L.: Nanolubrication by ionic liquids: molecular dynamics simulations reveal an anomalous effective rheology. Phys. Chem. Chem. Phys. **17**(35), 23226–23235 (2015)

[156] Fajardo, O.Y., Bresme, F., Kornyshev, A.A., Urbakh, M.: Water in ionic liquid lubricants: friend and foe. ACS nano **11**(7), 6825–6831 (2017)

[157] Bahrami, M., Ghatee, M.H., Ayatollahi, S.F.: Simulation of wetting and interfacial behavior of quaternary ammonium and phosphonium ionic liquid nanodroplets over face-centered cubic metal surfaces. J. Phys. Chem. B **124**(14), 2835–2847 (2020)

[158] Wang, Y.-L., Golets, M., Li, B., Sarman, S., Laaksonen, A.: Interfacial structures of trihexyltetradecylphosphonium-bis (mandelato) borate ionic liquid confined between gold electrodes. ACS Appl. Mater. Interfaces **9**(5), 4976–4987 (2017)

[159] Alexander, J.S., Maxwell, C., Pencer, J., Saoudi, M.: Equilibrium molecular dynamics calculations of thermal conductivity: A "how-to" for the beginners. CNL Nuclear Review **9**(1), 11–25 (2020)

[160] Müller-Plathe, F.: A simple nonequilibrium molecular dynamics method for calculating the thermal conductivity. J. Chem. Phys. **106**(14), 6082–6085 (1997)

[161] Salanne, M., Marrocchelli, D., Merlet, C., Ohtori, N., Madden, P.A.: Thermal conductivity of ionic systems from equilibrium molecular dynamics. J. Phys.: Condens. Matter **23**(10), 102101 (2011)

[162] Ishii, Y., Sato, K., Salanne, M., Madden, P.A., Ohtori, N.: Thermal conductivity of molten alkali metal fluorides (lif, naf, kf) and their mixtures. J. Phys.

Chem. B **118**(12), 3385–3391 (2014)

[163] Awad, A.N., Mohammed, S.S.: A study of enhancement of the properties of lubricant oil. Am. J. Chem. **4**(1), 68–72 (2014)

[164] Shah, J.K., Brennecke, J.F., Maginn, E.J.: Thermodynamic properties of the ionic liquid 1-n-butyl-3-methylimidazolium hexafluorophosphate from monte carlo simulations. Green Chem. **4**(2), 112–118 (2002)

[165] Androulaki, E., Vergadou, N., Ramos, J., Economou, I.G.: Structure, thermodynamic and transport properties of imidazolium-based bis (trifluoromethylsulfonyl) imide ionic liquids from molecular dynamics simulations. Mol. Phys. **110**(11-12), 1139–1152 (2012)

[166] Konieczny, J.K., Szefczyk, B.: Structure of alkylimidazolium-based ionic liquids at the interface with vacuum and water: A molecular dynamics study. J. Phys. Chem. B **119**(9), 3795–3807 (2015)

[167] AlTuwaim, M.S., Alkhaldi, K.H., Al-Jimaz, A.S., Mohammad, A.A.: Temperature dependence of physicochemical properties of imidazolium-, pyroldinium-, and phosphonium-based ionic liquids. J. Chem. Eng. Data **59**(6), 1955–1963 (2014)

[168] Bhattacharjee, A., Lopes-da-Silva, J.A., Freire, M.G., Coutinho, J.A., Carvalho, P.J.: Thermophysical properties of phosphonium-based ionic liquids. Fluid Phase Equilib. **400**, 103–113 (2015)

[169] Rivera, N., García, A., Fernández-González, A., Blanco, D., González, R., Battez, A.H.: Tribological behavior of three fatty acid ionic liquids in the lubrication of different material pairs. J. Mol. Liq. **296**, 111858 (2019)

[170] Fajardo, O., Bresme, F., Kornyshev, A., Urbakh, M.: Electrotunable lubricity with ionic liquid nanoscale films. Sci. Rep. **5**(1), 1–7 (2015)

[171] Fajardo, O.Y., Bresme, F., Kornyshev, A.A., Urbakh, M.: Electrotunable friction with ionic liquid lubricants: how important is the molecular structure of the ions? J. Phys. Chem. Lett. **6**(20), 3998–4004 (2015)

[172] Gerber, P.R.: Charge distribution from a simple molecular orbital type calculation and non-bonding interaction terms in the force field mab. J. Comput.-Aided Mol. Des. **12**(1), 37–51 (1998)

[173] Breneman, C.M., Wiberg, K.B.: Determining atom-centered monopoles from molecular electrostatic potentials. the need for high sampling density in formamide conformational analysis. J. Comput. Chem. **11**(3), 361–373 (1990)

Table 1 Density (g/cc) calculated using simulations (Sim) with different potentials at different temperature (Temp, K) compared to data from experiments (Exp) with the difference between them reported as error (%).

IL	Temp	Exp	Sim	Error	Potential	Reference
[P1,1,1,6][Tf_2N]	298	1.34	1.43	6.7	AMBER	[62]
[P2,2,2,1O1][Tf_2N]	298	1.42	1.46	2.8	AMBER	[62]
[P2,2,2,2O1][Tf_2N]	298	1.39	1.44	3.6	AMBER	[62]
[P2,2,2,5][Tf_2N]	298	1.32	1.3	1.5	APPLE&P	[33]
[P2,2,2,5][Tf_2N]	298	1.32	1.35	2.3	AMBER	[62]
[P2,2,2,8][Tf_2N]	298	1.26	1.28	1.6	AMBER	[62]
[P2,2,2,12][Tf_2N]	298	1.21	1.21	0	AMBER	[62]
[P4,4,4,14][Tf_2N]	298	1.125	1.12	1.2	AMBER	[62]
[P6,6,6,14][Tf_2N]	293	1.137	1.083	4.8	AMBER	[61]
[P8,8,8,8][Tf_2N]	298	1.076	1.07	0.5	AMBER	[62]
[P4,4,4,4][2-CNpyr]	333 - 413		0.896 - 0.845		GAFF	[85]
[P4,4,4,4][2-CNpyr-CO_2]	333 - 413		0.958 - 0.908		GAFF	[85]
[P4,4,4,4][BnIm]	333 - 413		0.921 - 0.873		GAFF	[85]
[P4,4,4,4][BnIm-CO_2]	333 - 413		0.981 - 0.931		GAFF	[85]
[P4,4,4,4][BrBnIm]	333 - 413		1.074 - 1.018		GAFF	[85]
[P4,4,4,4][BrBnIm-CO_2]	333 - 413		1.121 - 1.067		GAFF	[85]
[P4,4,4,4][CF_3Pyra]	333 - 413		0.969 - 0.913		GAFF	[85]
[P4,4,4,4][CF_3Pyra-CO_2]	333 - 413		1.02 - 0.964		GAFF	[85]
[P4,4,4,4][Im]	333 - 413		0.889 - 0.839		GAFF	[85]
[P4,4,4,4][Im-CO_2]	333 - 413		0.95 - 0.899		GAFF	[85]
[P4,4,4,4][Leu]	298	0.9269	0.924	0.3	AMBER	[50]
[P4,4,4,4][Ile]	298	0.9296	0.927	0.3	AMBER	[50]
[P4,4,4,4][Ala]	298	0.95	0.942	0.8	AMBER	[50]
[P4,4,4,4][Phe]	298	0.9524	0.98	2.9	AMBER	[50]
[P4,4,4,4][β-Ala]	298	0.959	0.954	0.5	AMBER	[50]
[P1,1,1,1][Gly]	300		1.392		GAFF	[72]
[P1,1,1,1][Gly]+10%H_2O	300		1.388		GAFF	[72]
[P4,4,4,4][Gly]	300	0.963	0.976	1.3	ReaxFF	[67]
[P4,4,4,4][Gly-CO_2]	300		1.000-1.049		ReaxFF	[67]
[P4,4,4,4][Gly]	300	0.963	0.993	3.0	GAFF	[72]
[P4,4,4,4][Gly]+10%H_2O	300		0.99		GAFF	[72]
[P4,4,4,4][Gly]	298	0.963	0.954	0.9	AMBER	[50]
[P4,4,4,4][Lys]	298	0.973	0.962	1.1	AMBER	[50]
[P4,4,4,4][Pro]	298	0.9828	0.963	2.0	AMBER	[50]
[P4,4,4,4][Met]	298	0.9868	0.984	0.3	AMBER	[50]
[P4,4,4,4][Ser]	298	0.991	0.993	0.2	AMBER	[50]
[P4,4,4,4][Glu]	298	1.0121	1.018	0.6	AMBER	[50]
[P4,4,4,4][Asp]	298	1.0173	1.028	1.1	AMBER	[50]
[P4,4,4,4][Tau]	298	1.0199	1.037	1.7	AMBER	[50]
[P4,4,4,4][Gln]	298	1.0519	1.003	4.6	AMBER	[50]
[P4,4,4,8][BMB]	293 - 373	1.0642 - 1.0084	1.0589 - 1.0118	0.5 - 0.3	A&D [1]	[35]
[P4,4,4,14][BMB]	293 - 373	1.0413 - 0.9841	1.0228 - 0.9789	1.8 - 0.5	A&D	[35]
[P6,6,6,14][BMB]	293 - 373	1.0086 - 0.9608	0.9979 - 0.9511	1.1 - 1.0	A&D	[35]
[P4,4,4,8][BScB]	293 - 373	1.0791 - 1.0219	1.0798 - 1.0312	0.1 - 0.9	A&D	[35]
[P4,4,4,14][BScB]	293 - 373	1.0405 - 0.9932	1.0472 - 1.0074	0.6 - 1.4	A&D	[35]
[P6,6,6,14][BScB]	293 - 373	1.0205 - 0.9633	1.0151 - 0.9854	0.5 - 2.3	A&D	[35]
[P4,4,4,8][BMLB]	293 - 373		1.1006 - 1.0578		A&D	[35]
[P4,4,4,14][BMLB]	293 - 373		1.0498 - 1.0011		A&D	[35]
[P6,6,6,14][BMLB]	293 - 373	0.9734 - 0.9265	1.0107 - 0.9683	3.8 - 4.5	A&D	[35]
[P4,4,4,8][BOB]	293 - 373		1.1034 - 1.0601		A&D	[35]
[P4,4,4,14][BOB]	293 - 373		1.0581 - 1.0105		A&D	[35]
[P6,6,6,14][BOB]	293 - 373	0.9973-0.9579 [2]	1.0215 - 0.9874		A&D	[35]
[P6,6,6,14][BOB]	298	0.97	1.01	4.1	A&D	[86]
[P4,4,4,8][Cl]	293 - 343	0.927 - 0.899	0.936 - 0.904	0.9 - 0.5	CL&P	[87]
[P6,6,6,14][Cl]	293	0.882	0.862	1.8	CL&P	[52]
[P6,6,6,14][Cl]	293	0.882	0.846	4.1	GAFF	[52]
[P6,6,6,14][Cl]	293 - 343	0.901 - 0.867	0.892 - 0.864	0.9 - 0.4	CL&P	[87]
[P6,6,6,14][Cl]	298	0.878	0.871	0.8	OPLS/CL&P	[41]
[P6,6,6,14][AcO]	293 - 333	0.902 - 0.875	0.895 - 0.870	0.8 - 0.5	CL&P&OPLS	[87]
[P6,6,6,14][Br]	298	0.958	0.938	2.2	OPLS/CL&P	[41]
[P6,6,6,14][Br]	298	0.958	0.942	1.7	OPLS/CL&P	[88]
[P6,6,6,14][DCA]	298	0.902	0.893	1.0	OPLS/CL&P	[88]
[$HP(Oct)_3$][TFO]	393 -465		0.884 - 0.836		OPLS	[89]
[$HP(Ph)_3$][TFO]	393 -465		1.19 - 1.123		OPLS	[89]

[1] A&D represents for AMBER&DREIDING.

[2] Exp density 293 - 353 K [90].

Table 2 Viscosity (mPa·s) calculated using simulations (Sim) with different potentials and calculation methods at different temperatures (Temp, K) compared to data from experiment (Exp) with the difference between them reported as error (%).

IL	Temp	Exp	Sim	Error	Potential	Method	Reference
[P2,2,2,2O1][Tf_2N]	400	3.8	4.1	7.9	AMBER	Green-Kubo	[65]
[P2,2,2,5][Tf_2N]	298	88	80	9.0	APPLE&P	Einstein	[33]
[P2,2,2,5][Tf_2N]	373	5.38	4.98	7.4	OPLS	Einstein	[107]
[P2,2,2,8][Tf_2N]	373	7.49	6.06	19.1	OPLS	Einstein	[107]
[P2,2,2,12][Tf_2N]	373		8.36		OPLS	Einstein	[107]
[P2,2,2,2][PhO]	298 - 420		1.76 - 0.77		OPLS/CL&P	Green-Kubo	[110]
[P3,3,3,3][PhO]	298 - 420		2.09 - 0.83		OPLS/CL&P	Green-Kubo	[110]
[P4,4,4,4][PhO]	298 - 420		2.01 - 0.94		OPLS/CL&P	Green-Kubo	[110]
[P6,6,6,6][PhO]	298 - 420		1.71 - 0.96		OPLS/CL&P	Green-Kubo	[110]
[P8,8,8,8][PhO]	298 - 420		1.15 - 0.98		OPLS/CL&P	Green-Kubo	[110]
[P6,6,6,14][Cl]	323	402	300	25.4	AMBER	Green-Kubo	[64]
[P6,6,6,14][Cl]	343	167	130	22.1	AMBER	Green-Kubo	[64]
[P6,6,6,14][Cl]	363	86	62	27.9	AMBER	Green-Kubo	[64]
[P6,6,6,14][Cl]	383	48	31	35.4	AMBER	Green-Kubo/NEMD	[64]
[P6,6,6,14][Cl]	403	29	13.5	53.4	AMBER	Green-Kubo	[64]
[P6,6,6,14][Cl]	423	18	9.5	47.2	AMBER	Green-Kubo/NEMD	[64]
[P6,6,6,14][Cl]	463	9	4.6	48.9	AMBER	Green-Kubo/NEMD	[64]
[P6,6,6,14][BMB]	373	67	75	11.9	AMBER	Green-Kubo	[64]
[P6,6,6,14][BMB]	383	47	68	44.7	AMBER	Green-Kubo	[64]
[P6,6,6,14][BMB]	403	27	29	7.4	AMBER	Green-Kubo	[64]
[P6,6,6,14][BMB]	423	18	16	11.1	AMBER	Green-Kubo/NEMD	[64]
[P6,6,6,14][BMB]	443	14	12	14.2	AMBER	Green-Kubo	[64]
[P6,6,6,14][BMB]	463	11	6	45.4	AMBER	Green-Kubo	[64]
[P6,6,6,14][Im]	298	810.4	897	11	OPLS	NEMD	[109]
[P6,6,6,14][ImC]	298	648.7	516.9	20	OPLS	NEMD	[109]
[P6,6,6,14][Tf_2N]	273		994.24		AMBER	Einstein	[61]
[P6,6,6,14][Tf_2N]	293	450	735.74	63.5	AMBER	Einstein	[61]
[P6,6,6,14][Tf_2N]	373		201.54		AMBER	Einstein	[61]
[P6,6,6,14][Tf_2N]	473		24.15		AMBER	Einstein	[61]
[P6,6,6,14][Tf_2N]	573		4.91		AMBER	Einstein	[61]
[$HP(Oct)_3$][TFO]	393		33.1		OPLS	Green-Kubo	[89]
[$HP(Oct)_3$][TFO]	417		25.2		OPLS	Green-Kubo	[89]
[$HP(Oct)_3$][TFO]	441		8.8		OPLS	Green-Kubo	[89]
[$HP(Oct)_3$][TFO]	465		6.6		OPLS	Green-Kubo	[89]
[$HP(Ph)_3$][TFO]	393		14.8		OPLS	Green-Kubo	[89]
[$HP(Ph)_3$][TFO]	417		9.3		OPLS	Green-Kubo	[89]
[$HP(Ph)_3$][TFO]	441		4.8		OPLS	Green-Kubo	[89]
[$HP(Ph)_3$][TFO]	465		3.6		OPLS	Green-Kubo	[89]
[$P2(Ph)_3$][PhO]	298 - 420		2.46 - 1.14		OPLS/CL&P	Green-Kubo	[110]
[$P3(Ph)_3$][PhO]	298 - 420		2.33 - 1.2		OPLS/CL&P	Green-Kubo	[110]
[$P4(Ph)_3$][PhO]	298 - 420		2.5 - 1.15		OPLS/CL&P	Green-Kubo	[110]
[$P6(Ph)_3$][PhO]	298 - 420		2.56 - 1.17		OPLS/CL&P	Green-Kubo	[110]
[$P8(Ph)_3$][PhO]	298 - 420		1.22 - 1.12		OPLS/CL&P	Green-Kubo	[110]

Table 3 Self-diffusion coefficient ($10^{-12}m^2/s$) of cations and anions calculated using simulations (Sim) with different potentials at different temperatures (Temp, K).

IL	Temp	Cation	Anion	Potential	Reference
[P2,2,2,2O1][Tf_2N]	400	410	450	AMBER	[65]
[P2,2,2,5][Tf_2N]	298	8.5	10.1	APPLE&P	[33]
[P2,2,2,5][Tf_2N]	373	29.2	34.8	OPLS/CL&P	[107]
[P2,2,2,8][Tf_2N]	373	20	30.2	OPLS/CL&P	[107]
[P2,2,2,12][Tf_2N]	373	13.9	20.8	OPLS/CL&P	[107]
[P6,6,6,14][Tf_2N]	298 - 398	1.33 - 14.37	1.45 - 10.75	CL&P	[52]
[P6,6,6,14][Tf_2N]	273 - 573	2.08 - 421.44	2.08 - 421.44	AMBER	[61]
[P4,4,4,8][BMB]	333	2.634	3.237	A&D [1]	[35]
[P4,4,4,14][BMB]	333	2.066	2.711	A&D	[35]
[P6,6,6,14][BMB]	333	2.737	3.215	A&D	[35]
[P4,4,4,8][BMLB]	333	1.648	1.825	A&D	[35]
[P4,4,4,14][BMLB]	333	1.78	2.588	A&D	[35]
[P6,6,6,14][BMLB]	333	2.645	2.818	A&D	[35]
[P4,4,4,8][BOB]	333	2.079	3.63	A&D	[35]
[P4,4,4,14][BOB]	333	5.521	7.357	A&D	[35]
[P6,6,6,14][BOB]	333	2.054	2.254	A&D	[35]
[P4,4,4,8][BScB]	333	3.28	3.431	A&D	[35]
[P4,4,4,14][BScB]	333	2.645	2.851	A&D	[35]
[P6,6,6,14][BScB]	333	3.073	4.178	A&D	[35]
[P2,2,2,2][PhO]	298 - 420	37 - 611	36.7 - 827	OPLS/CL&P	[110]
[P3,3,3,3][PhO]	298 - 420	5.1 - 371	6.5 - 532	OPLS/CL&P	[110]
[P4,4,4,4][PhO]	298 - 420	1.2 - 161	2.1 - 269	OPLS/CL&P	[110]
[P6,6,6,6][PhO]	298 - 420	0.9 - 67	1.3 - 122	OPLS/CL&P	[110]
[P8,8,8,8][PhO]	298 - 420	0.7 - 32	1.1 - 42	OPLS/CL&P	[110]
[$P2(Ph)_3$][PhO]	298 - 420	0.9 - 221	1.0 - 265	OPLS/CL&P	[110]
[$P3(Ph)_3$][PhO]	298 - 420	0.5 - 147	0.9 - 191	OPLS/CL&P	[110]
[$P4(Ph)_3$][PhO]	298 - 420	0.5 - 128	1.2 - 209	OPLS/CL&P	[110]
[$P6(Ph)_3$][PhO]	298 - 420	0.5 - 100	0.9 - 182	OPLS/CL&P	[110]
[$P8(Ph)_3$][PhO]	298 - 420	1.3 - 81	1.5 - 179	OPLS/CL&P	[110]
[P4,4,4,4][BnIm]	413	45.3	75.1	Class I	[85]
[P4,4,4,4][BnIm]+H_2O	413	47.5	89.9	Class I	[85]
[P4,4,4,4][BnIm-CO_2]	413	43.2	66.6	Class I	[85]
[P4,4,4,4][BnIm-CO_2]+H_2O	413	45.1	68.3	Class I	[85]
[P4,4,4,4][2-CNpyr]	333 - 413	8.6 - 99.6	13.1 - 150.6	GAFF	[51]
[P4,4,4,4][2-CNpyr]	413	78.5	145.4	Class I	[85]
[P4,4,4,4][2-CNpyr]+H_2O	413	95.4	161.5	Class I	[85]
[P4,4,4,4][2-Cnpyr-CO_2]	413	67.3	102.3	Class I	[85]
[P4,4,4,4][2-Cnpyr-CO_2]+H_2O	413	69.6	103.4	Class I	[85]
[P2,2,2,8][2-CNpyr]	333	33	47	Class I	[117]
[P2,2,2,8][2-CNpyr]+H_2O	333	44	70	Class I	[117]
[P2,2,2,8][3Triaz]	333	13	13	Class I	[117]
[P2,2,2,8][3Triaz]+H_2O	333	22	37	Class I	[117]
[P2,2,2,8][PhO]	333	26	30	Class I	[117]
[P2,2,2,8][PhO]+H_2O	333	23	34	Class I	[117]
[P1,1,1,1][Gly]	300	0.2	0.2	AMBER	[72]
[P1,1,1,1][Gly]+H_2O	300	0.3	0.2	AMBER	[72]
[P4,4,4,4][Gly]	300	0.8	0.7	AMBER	[72]
[P4,4,4,4][Gly]+H_2O	300	0.7	0.8	AMBER	[72]

[1] A&D represents for AMBER&DREIDING.

Table 4 Ionic conductivity (S/c) calculated using simulations (Sim) with different potentials at different temperatures (Temp, K) and compared to data from experiments (Exp) and the difference between them reported as error (%).

IL	Temp	Exp	Sim	Error	Potential	Reference
[P2,2,2,5][Tf_2N]	298	0.00173	0.00134	23%	APPLE&P	[33]
[P2,2,2,5][Tf_2N]	298 -361		0.0021 - 0.01169		AMBER	[71]
[P2,2,2,5][Tf_2N]	373		0.0192		OPLS/CL&P	[107]
[P2,2,2,8][Tf_2N]	373		0.0151		OPLS/CL&P	[107]
[P2,2,2,12][Tf_2N]	373		0.0104		OPLS/CL&P	[107]
[Li]0.25[P2,2,2,2O1]0.75[Tf_2N]	298 -361		0.000612 - 0.00721		AMBER	[71]
[Li]0.39[P2,2,2,2O1]0.61[Tf_2N]	298 -361		0.000159 - 0.00353		AMBER	[71]
[P2,2,2,2O1][Tf_2N]	400 K	0.0302	0.0425	40%	AMBER	[65]
[P2,2,2,2O1][Tf_2N]	298 -361		0.00384 - 0.0184		AMBER	[71]
[Li]0.25[P2,2,2,2O1]0.75[Tf_2N]	298 -361		0.00142 - 0.01177		AMBER	[71]
[Li]0.39[P2,2,2,2O1]0.61[Tf_2N]	298 -361		0.00037 - 0.00501		AMBER	[71]
[P6,6,6,14][Tf_2N]	273 -573		0.000002 - 0.000383		AMBER	[61]
[HP($Oct)_3$][TFO]	393 - 465 K		0.00045 - 0.0044		OPLS	[89]
[HP($Ph)_3$][TFO]	393 - 465 K		0.002- 0.0138		OPLS	[89]

Table 5 Heat capacity (J/(K·g)) calculated using simulations (Sim) with different potentials at different temperatures (Temp, K) and compared to data from experiment (Exp) and the difference between them reported as error (%).

IL	Temp	Exp	Sim	Error	Potential	Reference
[P4,4,4,4][Lys]	310	1.8434	2.63405	42.9	AMBER	[50]
[P4,4,4,4][Lys]	310	2.5198	2.63405	4.4	AMBER	[125]
[P4,4,4,4][Gly]	310	2.1422	2.52506	17.8	AMBER	[50]
[P4,4,4,4][Gln]	310	2.1748	2.41312	11.0	AMBER	[50]
[P4,4,4,4][Glu]	310	2.2223	2.4051	8.2	AMBER	[50]
[P4,4,4,4][Pro]	310	2.2336	2.4931	11.6	AMBER	[50]
[P4,4,4,4][Tau]	310	2.2403	2.46605	10.1	AMBER	[50]
[P4,4,4,4][Ile]	310	2.3186	2.51507	8.5	AMBER	[50]
[P4,4,4,4][Leu]	310	2.3591	2.56406	8.7	AMBER	[50]
[P4,4,4,4][Ser]	310	2.3599	2.46806	4.6	AMBER	[50]
[P4,4,4,4][Met]	310	2.4424	2.47605	1.4	AMBER	[50]
[P4,4,4,4][Ala]	310	2.4582	2.58707	5.2	AMBER	[50]
[P4,4,4,4][β-Ala]	310	2.4577	2.66508	8.4	AMBER	[50]
[P4,4,4,4][Asp]	310		2.45209		AMBER	[50]
[P4,4,4,4][Phe]	310	2.6112	2.41506	7.5	AMBER	[50]
[P4,4,4,4][2-CNpyr]	333 - 413		2.237		GAFF	[51]
[P4,4,4,4][2-CNpyr-CO_2]	333 - 413		2.396		GAFF	[51]
[P6,6,6,14][Tf_2N]	273 - 573	1.79 - 2.04	2.078	8.3	AMBER	[61]